Selecting crop models for decision making in wheat insurance

A. Castañeda-Vera , P.A. Leffelaar , J. Álvaro-Fuentes , C. Cantero-Martínez , M.I. Mínguez

Keywords:
Aquacrop
CERES-Wheat
CropSyst
WOFOST
Model choice
Rainfed semi-arid areas
Radiation use efficiency
Water deficit

A B S T R A C T

In crop insurance, the accuracy with which the insurer quantifies the actual risk is highly dependent on the availability on actual yield data. Crop models might be valuable tools to generate data on expected yields for risk assessment when no historical records are available. However, selecting a crop model for a specific objective, location and implementation scale is a difficult task. A look inside the different crop and soil modules to understand how outputs are obtained might facilitate model choice. The objectives of this paper were (i) to assess the usefulness of crop models to be used within a crop insurance analysis and design and (ii) to select the most suitable crop model for drought risk assessment in semi-arid regions in Spain. For that purpose first, a pre-selection of crop models simulating wheat yield under rainfed growing conditions at the field scale was made, and second, four selected models (Aquacrop, CERES-Wheat, CropSyst and WOFOST) were compared in terms of modelling approaches, process descriptions and model outputs. Outputs of the four models for the simulation of winter wheat growth are comparable when water is not limiting, but differences are larger when simulating yields under rainfed conditions. These differences in rainfed yields are mainly related to the dissimilar simulated soil water availability and the assumed linkages with dry matter formation. We concluded that for the simulation of winter wheat growth at field scale in such semi-arid conditions, CERES-Wheat and CropSyst are preferred. WOFOST is a satisfactory compromise between data availability and complexity when detail data on soil is limited. Aquacrop integrates physiological processes in some representative parameters, thus diminishing the number of input parameters, what is seen as an advantage when observed data is scarce. However, the high sensitivity of this model to low water availability limits its use in the region considered. Contrary to the use of ensembles of crop models, we endorse that efforts be concentrated on selecting or rebuilding a model that includes approaches that better describe the agronomic conditions of the regions in which they will be applied. The use of such complex methodologies as crop models is associated with numerous sources of uncertainty, although these models are the best tools available to get insight in these complex agronomic systems.

1. Introduction

Crop models are essential tools to understand the complexity of cropping systems since they compile knowledge on physiological processes and plant interactions with the environment, which are deemed crucial. In research, models are used to address research problems and interpret experimental results (Rinaldi et al., 2007), to evaluate the impact of alternative management strategies on production (Ventrella et al., 2012) and on the environment (Asseng et al., 1998a), to investigate crop production levels (Van Ittersum et al., 2013) or to predict yields under changing climatic conditions (Asseng et al., 2013). Also in decision-making, crop models are increasingly used, for example, for policy shaping and analysis

(e.g. CAP greening measures), farmer consultancy (e.g. Hunt et al., 2006) or risk management with early warning systems (e.g. Basso et al., 2013).

In crop insurance, risk is defined as the probability of registering a claim; in the case of drought insurance, a claim is registered when actual yield is lower than the insured yield. Consequently, risk depends on yield variability. The calculated risk is used to set and update premiums, or to design new insurance policies. The accuracy with which the insurer quantifies the actual risk is highly dependent on the availability on high quality actual yield data. However, records on observed yields are not always complete, and the information available for the insurer to calculate the probability and severity of a claim can be biased. This can give rise to unbalanced loss ratios, thereby affecting the actuarial robustness and sustainability of entire insurance systems. In these cases, crop models might be valuable tools to generate data on expected yields for risk assessment when no historical data is available.

However, the uncertainty associated with the use of crop models is large. Many crop and soil water models exist. They differ in aspects such as parameter requirements, time coefficient, simulation of the spatial scale or their either more process-based or more empirically based approach (e.g., Angulo et al., 2014; Kersebaum et al., 2007). Model complexity, the scale of application and the availability of data for model calibration and validation affect the reliability of simulations, especially when simulation purposes differ from those for which the selected model was designed (Kersebaum et al., 2007). In rainfed cropping systems in semi-arid areas, crops are highly dependent on soil moisture along the cropping cycle. The precision of soil water modules in simulating soil water dynamics and the capacity of the crop modules to translate the effects of water stress on crop canopy and biomass growth have an impact on the accuracy of simulated yields. Therefore, crop models should be used with caution, particularly when applied to more resource-limited conditions and when used in decision support systems where environmental, social and economic assets are involved.

Asseng et al. (2013) found a larger uncertainty related to crop models than related to climate models when simulating under future climate projections, and that variation of simulated yield was larger for low-yielding environments. Furthermore, Martre et al. (2014) studied two ensemble-based crop models and concluded that taking the mean or the median of the simulated values estimates better than any single crop model simulations.

Subsequently, a number of questions arise: (i) Which model(s) is/are preferred from the investigated models? (ii) Is the use of the average of several model's outputs better than the use of a single model output? (iii) Given the uncertainties associated to crop model simulations, is it possible to responsibly use crop models in crop insurance analysis and design? And what precautions should be taken when using crop model simulations for decision making regarding model(s) calibration and implementation?

The objectives of this paper were (i) to assess the usefulness of crop models to be used within a crop insurance analysis and design and (ii) to select the most suitable crop model for drought risk assessment in semi-arid regions in Spain. For that purpose first, a pre-selection of crop models simulating wheat yield under rainfed growing conditions at the field scale was made, and second, four selected models were compared in terms of modelling approaches, process description and model outputs. Each selected model calculates aboveground biomass accumulation and soil water balance using different approaches. Likewise, they use alternative assumptions to compute the effect of daily water stress on crop and biomass production. The four crop models were run for winter wheat (*Triticum aestivum* L.) over five growing seasons in NE Spain.

2. Materials and methods

2.1. Models

Four models were pre-selected from the 27 wheat simulation models included in the AgMIP wheat study (Asseng et al., 2013; Martre et al., 2014). The criteria to select them were having (i) a comparable structure in terms of submodules; (ii) different approaches to calculate the daily accumulation of biomass; (iii) different approaches to calculate the daily change in soil water content; and (iv) different approaches to calculate the penalties on crop growth due to water deficit. From all models meeting these criteria, the four more widely used in Spanish conditions were selected: Aquacrop (Raes et al., 2009; Steduto et al., 2012), CSM-CROPSIM-CERES-Wheat (hereafter referred to as CERES-Wheat), available in the package Decision Support System for Agrotechnology Transfer (DSSAT) version 4.5 (Hoogenboom et al., 2012; Jones et al., 2003), CropSyst (Stöckle et al., 2003) and WOFOST (Boogaard et al., 2011; Supit et al., 1994).

With respect to the approach used to calculate the daily accumulation of biomass, Aquacrop calculates biomass production based on water availability through a transpirational water use efficiency coefficient (WUE, g biomass mm^{-1}); CERES-Wheat calculates biomass production rate based directly on radiation through a radiation use efficiency coefficient (RUE, g biomass MJ^{-1}); CropSyst combines the last two approaches, RUE and WUE; and, lastly, WOFOST calculates biomass production rate based on the net carbon assimilation by subtracting maintenance and respiration requirements from gross assimilation of CO_2 (Table 1).

The approaches used to calculate the daily change in soil water content are also different. Aquacrop uses a cascade approach (when no groundwater table is considered as is the case for the semi-arid Spanish regions) that is computed on a 12 layers-subdivided soil; CERES-Wheat uses a cascade approach with potential capillary rise calculated based on soil water diffusivity with a user-defined soil subdivision in layers; in CropSyst, the finite difference approach based on Richard's equation computed on a 20 layers-subdivided soil was selected; and, finally, WOFOST uses a cascade approach (when no groundwater table is considered) that is computed for a homogeneous soil of a single layer. The four models all have submodels for phenology and canopy development, for growth and biomass partitioning, and for the soil water balance.

The differences between the models are found in the detail of the different submodels. Main characteristics of the models are summarized in Tables 1 and 2, and most important equations and approaches are described in detail below.

2.1.1. Aboveground biomass production

CERES-Wheat calculates biomass production rate based directly on radiation through a radiation use efficiency coefficient (RUE, g biomass MJ^{-1}). Aquacrop calculates biomass production based on water availability through a transpirational water use efficiency coefficient (WUE, g biomass mm^{-1}). CropSyst combines the last two approaches, RUE and WUE. Lastly, WOFOST calculates biomass production rate based on the net carbon assimilation by subtracting maintenance and respiration requirements from gross assimilation of CO_2.

Aquacrop computes the daily aboveground biomass (AgB) production $\left(\frac{dAgB}{dt}\text{kg ha}^{-1}\text{ day}^{-1}\right)$ from the potential daily biomass production $\left(\frac{dAgB}{dt}_{POT}\text{kg ha}^{-1}\text{ day}^{-1}\right)$, the so-called water productivity coefficient (*WP*) (given as an input parameter), and the ratio of actual to reference evapotranspiration:

$$\frac{dAgB}{dt} = WP \times \left(\frac{Ta}{ET_o}\right) \quad (1)$$

Table 1
Main characteristics of Aquacrop, CERES-Wheat, CropSyst and WOFOST and the computation of water stress.

		Aquacrop	CERES-Wheat	CROPSYST	WOFOST
	Biomass accumulation	WUE[a]	RUE[a]	RUE and WUE	CO_2 assimilation, maintenance and respiration
	Yield formation	AgB, HI[b]	AgB, grains number and grain weight	AgB, HI	AgB, partitioning coefficients
	Roots modelling	Depth	Density and depth	Fraction per soil layer and depth	Depth
	Water uptake (Ta)	RAW[c] in the soil layer and soil depth	RAW and root density per layer	DWP[d] crop–soil and root fraction per layer	RAW in the root zone
Water deficit effect on	Phenology	Early CC[e] senescence	No	Accelerate the accumulation of °C-days	No
	AgB	↓[f]Ta[g] → ↓(*dAgB*)/*dt* ↓CC → ↓Ta → ↓(*dgB*)*dt*	↓Ta → ↓(*dAgB*)*dt*	↓Ta → ↓(*dAgB*)/*dt*	↓Ta → ↓(*dAgB*)/*dt*
	Partitioning	Modifies harvest index	Induces root growth Affects harvest index though sink size	Accelerates the accumulation of degree-days, hastening physiological maturity	No

[a] RUE: Radiation use efficiency; WUE: Water use efficiency.
[b] AgB: Aboveground biomass; HI: Harvest Index.
[c] RAW: Readily Available Water, between pF 4.2 (−1500 kPa) and pF 2.5 (−33 kPa).
[d] DWP: Differences in water potential.
[e] Canopy.
[f] ↓: decrease, ↑: increase.
[g] Ta: Actual transpiration; ↓(*dAgB*)/*dt*: Aboveground biomass production rate.

$$\frac{Ta}{ET_o} = K_s \times CC^* \times K_{C,Tr} \quad (2)$$

$$CC^* = \min(1, 1.72 \times CC - CC^2 + 0.3 \times CC^3) \quad (3)$$

where Ta is the actual transpiration (mm day^{-1}), ET_o is the reference evapotranspiration (mm day^{-1}), K_s is the water stress index (–), CC is the canopy cover (m^2 m^{-2}), CC^* is the adjusted canopy cover for micro-advective effects (m^2 m^{-2}) and $K_{C,Tr}$ (–) is the coefficient for maximum crop transpiration that corresponds with a well-watered soil and fully developed canopy ($CC = 1$).

In CERES-Wheat, $dAgB/dt_{POT}$ is calculated from the intercepted photosynthetically active radiation (*IPAR*, MJ ha^{-1} day^{-1}), that is previously calculated from the leaf area index (*LAI*, m^2 m^{-2}), a light extinction coefficient (k, –) and *PAR*, and the radiation use efficiency (*RUE*, kg AgB dry matter MJ^{-1}) ($dAgB/dt_{IPAR}$, kg ha^{-1} day^{-1}):

$$IPAR = PAR \times \left(1 - e^{-k \times LAI}\right) \quad (4)$$

$$\frac{dAgB}{dt}_{POT} = \frac{dAgB}{dt}_{IPAR} = RUE \times IPAR \quad (5)$$

where *PAR* is the photosynthetically active radiation (MJ ha^{-1} day^{-1}) (estimated as half of the global radiation).

In CropSyst, the $dAgB/dt_{POT}$ is calculated as proposed by Tanner and Sinclair (1983) based on the minimum of (i) the radiation dependent biomass growth, based on the photosynthetically active radiation intercepted by the crop ($dAgB/dt_{IPAR}$, kg ha^{-1} day^{-1}), and (ii) the transpiration dependent biomass growth ($dAgB/dt_{PT}$, kg ha^{-1} day^{-1}), relying on the estimate of potential crop transpiration:

$$\frac{dAgB}{dt}_{POT} = \min\left(\frac{dAgB}{dt}_{IPAR}, \frac{dAgB}{dt}_{PT}\right) \quad (6)$$

$$\frac{dAgB}{dt}_{PT} = K_{BT} \times \frac{T_P}{VPD} \times 10^{-3} \quad (7)$$

$$T_p = ET_p \times \left(1 - e^{-k \times GAI}\right) \quad (8)$$

where *RUE* is the radiation use efficiency to produce AgB (kg dry matter MJ^{-1}), K_{BT} is a biomass-transpiration coefficient under given conditions of atmospheric vapour pressure deficit (Pa kg biomass (kg water)$^{-1}$), *VPD* is the vapour pressure deficit (kPa), T_p is the potential daily crop transpiration (kg water ha^{-1} day^{-1}) and *GAI* is the green area index (m^2 m^{-2}). CropSyst distinguishes *LAI* from *GAI*, in which just the green photosynthetically active fraction of the canopy is included.

WOFOST initiates crop growth from calculating the carbon assimilation (A_t, kg CH_2O ha(leaf)$^{-1}$ h^{-1}):

$$A_t = A_{max} \times \left(1 - e^{-\varepsilon \times \frac{IPAR}{A_{max}}}\right) \quad (9)$$

where A_{max} is the maximum daily gross assimilation (kg CH_2O ha(leaf)$^{-1}$ h^{-1}), ε is the radiation use efficiency to produce assimilates in a single leaf (kg CH_2O ha(leaf)$^{-1}$ h^{-1} J^{-1} m^2 s) and *IPAR* is here expressed in J m^{-2} s^{-1}. The rate of assimilation by individual leaves is then transformed into the rate for the whole canopy using a three-point Gaussian integration method as a weighted average of the assimilate production rates at three levels within the canopy (Goudriaan, 1986). After extracting assimilates required for standing biomass maintenance (R_m, kg CH_2O ha(soil)$^{-1}$ h^{-1}), the rate of AgB production is computed by multiplying the left assimilates by a conversion coefficient (C_e, kg biomass kg^{-1} CH_2O):

$$\frac{dAgB}{dt} = 24 \times C_e \times (A_t \times LAI - R_m) \quad (10)$$

A_t is multiplied by *LAI* to convert the assimilation rate per ha of leaves into the rate per ha of soil and 24 transforms the hourly rate into a daily rate. C_e and R_m vary depending on the organ.

2.1.2. Canopy and crop development

Phenology is simulated in all four models based on thermal time. CERES-Wheat, CropSyst and WOFOST include also the influence of day length. CERES-Wheat and CropSyst include the effect of vernalization. Crop development has a major influence on final yield, especially in CERES-Wheat and WOFOST in which biomass is partitioned to yield just after the grain filling period starts. Therefore, the length of the grain filling period (from anthesis to physiological maturity) has an enormous effect on final yield. Phenology can be accelerated by water and/or temperature stresses.

Table 2
Main characteristics of the soil modules as used in Aquacrop, CERES-Wheat, CropSyst and WOFOST.

	Aquacrop	CERES-Wheat	CROPSYST	WOFOST
Approach	Finite difference No upflow if no groundwater table	Cascade with upflow based on soil water diffusivity	Finite difference, based on Richard' s equation	Cascade, no upflow if no groundwater table
Soil compartments	Subdivision with ΔZ increasing exponentially with depth, 12 nodes	User specified or subdivision with ΔZ increasing exponentially with depth	User specified (up to 20) or subdivision with ΔZ increasing exponentially with depth	One
Allows profile heterogeneity?	Yes	Yes	Yes	No
Potential ET	ET_o as input variable	$ET_o = \frac{0.408\Delta(R_n-G)+\gamma\frac{900}{T+273}(e_s-e_a)}{\Delta+\gamma(1+0.34u_z)}$	$ET_o = \frac{0.408\Delta(R_n-G)+\gamma\frac{900}{T+273}(e_s-e_a)}{\Delta+\gamma(1+0.34u_z)}$	$ET_o = \frac{\Delta}{\Delta+\gamma}R_{na} + \left(\frac{\gamma}{\Delta+\gamma}\right)E_{ac}$
Infiltration and drainage	$\frac{\partial\theta_t}{\partial t} = \tau\left(\theta_{SAT}-\theta_{FC}\right)\left[\left(\frac{e^{\theta_i-\theta_{FC}}-1}{e^{SAT-\theta_{FC}}-1}\right)\right]$ $\tau = 0.0866\times K_{sat}{}^{0.35} \le 1$	$\frac{\partial\theta_t}{\partial t} = K_{sat}(\theta_t-\theta_{FC})$	$\frac{\partial\theta_t}{\partial t} = K_{sat}(\theta_t-\theta_{FC})$	$\frac{\partial\theta_t}{\partial t} = K_{sat}(\theta_t-\theta_{FC})$ $\frac{\partial\theta_t}{\partial t} = P+I_e-E_w-\frac{SS_t}{\Delta t}$
Upflow	If a groundwater table is present: $\frac{\partial\theta_i}{\partial t} = e^{\frac{\ln(z)-b}{a}}$	$\frac{\partial\theta_i}{\partial t} = D(\theta)\times\frac{\theta_i-\theta_{i+1}}{(Z_i+Z_{i+1})\times 0.5}$ $D(\theta) = \begin{cases} 0.88, \theta_i \le LL \\ \max[100, 0.88\times e^{0.35\left(\frac{\theta_i}{2}+\frac{\theta_{i+1}}{2}\right)}], \theta_i > LL \end{cases}$	$\frac{\partial\theta_t}{\partial t} = \frac{\partial}{\partial t}\left[K(\theta)\left(\frac{\partial\varphi}{\partial z}+1\right)\right]$	If a groundwater table is present: $\frac{\partial\theta}{\partial t}_{\max} = \frac{W_{rz,fc}-W_r}{\Delta t}$ $W_{rz,fc} = RD\times\theta_{SAT}+\theta_{air}(z-RD)-\theta_{air}(z)$ $\theta_{air}(h) = \Delta\varphi\frac{\theta_{air,-1}+1.6\theta_{air,0}+\theta_{air,1}}{3.6}$
Soil evaporation	$U_{limit} = 1000\left(\theta_{FC}-\theta_{airdry}\right)Z_{evap}$ $\theta_{airdry} = 1/2\theta_{PWP}$ ***Stage I:*** $E_a = (1-CC^*)K_{ex}ET_o$ $K_{ex} = 1.1\,\mathrm{mm\,day^{-1}}$ ***Stage II:*** $E_a = K_r(1-CC^*)K_{ex}ET_o$ $0 \le K_r = \frac{e^{f_x W_{rel}}-1}{e^{f_x}-1} \le 1$	U_{limit} is use specified $\theta_{airdry} = 1/2\theta_{PWP}$ $E_{Eq} = R_n(0.00488-0.00437\alpha)(T_{mean}+29)$ $E_p = \begin{cases} E_{Eq}[(T_{max}-24)\times 0.05+1], T_{max} \ge 5°C \\ E_{Eq}\times 0.01e^{0.18(T_{max}+20)}, T_{max} < 5°C \end{cases}$ $E_{soil} = \begin{cases} E_p(1-0.43LAI), LAI < 1 \\ E_{Eq}e^{-0.4LAI}, LAI \ge 1 \end{cases}$ ***Stage I:*** $E_a = E_{soil}$ ***Stage II:*** $E_a = E_{soil}t^{-0.5}$	$E_p = (1-f_{Cres})\left(1-f_{Ccanopy}\right)ET_p\theta_{airdry} = 1/3\theta_{PWP}$ ***Stage I:*** $E_a = E_p$ ***Stage II:*** $E_a = E_p\frac{\theta_i-\theta_{airdry}}{\theta_{FC}-\theta_{airdry}}$	$E_{p,bare} = ET_o e^{-k_{gb}LAI}$ $E_{w,max} = EO_w e^{-k_{gb}LAI}$ $E_{s,max} = EO_s e^{-k_{gb}LAI}$ $\begin{cases} E_a = E_{w,max}\, if SS_t \ge 1cm \\ E_a = E_{s,max}\, if SS_t < 1cm and \frac{\partial\theta_i}{\partial t} \ge 1cm day^{-1} \\ E_a = E_{s,max}\left(\sqrt{D_{slr}}-\sqrt{D_{slr}-1}\right) if \frac{\partial\theta_i}{\partial t} < 1cm day^{-1} \end{cases}$
Runoff	Curve number method	Curve number method	Curve number method	$Runoff = SS_t - min(SS_t, SS_{max})$ $SS_t = SS_{t-1}+\left(P+I_e-E_w-\frac{\partial\theta_i}{\partial t}\right)\Delta t$

Table 2 (*Continued*)

Δ: Slope of the saturation vapour pressure curve (kPa °C^{-1}).
R_n: net radiation at the crop surface (MJ m^{-2} day^{-1}).
G: Soil heat flux density (MJ m^{-2} day^{-1}).
γ: Psychometric constant at the sea level (kPa °C^{-1}).
T: Daily average temperature (°C).
$e_s - e_a$: vapour pressure deficit (kPa).
u_z: wind speed at z m.
E_{ac}: Evaporative demand in equivalent evaporation (mm day^{-1}).
R_{na}: Net absorbed radiation in equivalent evaporation (mm day^{-1}).
θ_t, θ_{PWP} (~LL), θ_{FC}, θ_{SAT}, θ_{airdry}: Soil moisture content at time t, at permanent wilting point, at field capacity, at saturation and at air dry (cm^3 cm^{-3}).
$\theta_{air,h}$: Soil moisture content at time t, at selected matric head (h) (cm^3 cm^{-3} kPa^{-1}).
$W_{rz,fc}$, W_{rz}: Equilibrium and actual amount of water in the rooting zone (cm).
$\Delta\psi$: height of interval matric head (KPa).
τ: drainage characteristic (day^{-1}).
K_{sat}: Hydraulic conductivity at saturation (mm day^{-1}).
P: daily precipitation (mm day^{-1}).
I_e: effective irrigation (mm day^{-1}).
E_w: evaporation rate from a shaded water surface (mm day^{-1}).
a, b: parameters that depends on the soil layer textural class.
z: ground water table depth (m).
SS_{max}, SS_t: maximum surface water storage and at time t (mm).
$D(\theta)$: water diffusivity (cm day^{-1}).
EO_w, EO_s, $E_{p,bare}$: potential evaporation rate from a shaded water surface, from a shaded soil surface and from a bare soil (mm day^{-1}).
$E_{w,max}$, $E_{s,max}$: maximum evaporation rate from a shaded water surface and from a shaded soil (mm day^{-1}).
Z_l, Z_{l+1}: soil depth of soil layer l and subsequent layer $l+1$ (m).
θ_l, θ_{l+1}: soil moisture content of soil layer l and subsequent layer $l+1$ (cm^3 cm^{-3}).
RD: actual rooting depth (m).
U_{limit}: maximum water to be evaporated in the stage I (mm).
Z_{evap}: upper soil layer depth (m).
E_a, E_p E_{eq}: actual, potential and equilibrium soil evaporation rate (mm day^{-1}).
LAI: Leaf area index (m^2 m^{-2}).
K_{ex}: maximum soil evaporation coefficient.
CC^*: canopy cover adjusted by micro-advective effects (–).
f_x, W_{rel}: decline factor and relative wetness of the soil (–).
f_{Cres}, $f_{Ccanopy}$: fraction of incident radiation intercepted by the residues and by the canopy cover (0–1).
k_{gb}: extinction coefficient for solar radiation (–).
D_{slr}: days since last rain.
K_r: relative water content of the upper soil layer.

Potential daily biomass production is highly dependent on canopy development through *LAI* and *CC*, related to each other through the extinction coefficient (k) (Eq. (11)). *CC* is directly included in the computation of crop potential transpiration (Aquacrop) and intercepted radiation (CERES-Wheat, CropSyst and WOFOST).

$$CC = 1 - e^{-LAI \times k} \tag{11}$$

In Aquacrop, canopy development is calculated based on the actual canopy cover:

$$\begin{aligned} CC_t &= CC_o \times e^{CGC \times TT} && CC_t \leq 0.5CC_{max} \\ CC_t &= CC_{max} - 0.25 \times \left(\frac{{CC_{max}}^2}{CC_o} \right) \times e^{-CGC \times TT} && CC_t > 0.5CC_{max} \end{aligned} \tag{12}$$

and canopy decline:

$$CC_t = CC_{max} \times [1 - 0.005 \times (e^{\frac{CDC}{CC_{max}} \times TT} - 1)] \tag{13}$$

where CC_o, CC_t and CC_{max} are the initial, actual and maximum canopy cover (fraction of soil covered by the crop), and *CGC* is the canopy relative growth rate (°C-day^{-1}), *CDC* is the canopy decline rate (fraction soil covered °C-day^{-1}), and *TT* is the accumulated thermal time (°C-day). The beginning of canopy decline is determined developmentally at a specified thermal time that is set through a crop parameter.

In CERES-Wheat, leaf area of a plant is calculated as the product of the rate of leaf appearance and the rate of expansion of growing leaves. In this model, only leaf blade area is considered and it is assumed that just one leaf at a time is expanding on the stem. *LAI* is calculated by multiplying the accumulated leaf area per plant and the plant density (*PD*, plants m^{-2}):

$$\frac{dLAI}{dt} = \left(\frac{dLeafAreaExpansion}{dt}_{plant} - \frac{dLeafAreaLoss}{dt}_{plant} \right) \times PD \tag{14}$$

where $\frac{dLeafAreaExpansion}{dt}_{plant}$ is the daily growth of leaf area per plant (m^2 plant^{-1} day^{-1}), $\frac{dLeafAreaLoss}{dt}_{plant}$ is the daily senescence of leaf area (m^2 plant^{-1} day^{-1}). The accumulation of leaf area per plant is sink-dependent, depending on the number of tillers and leaves:

$$\frac{dLeafAreaExpansion}{dt}_{plant} = \frac{dLeafAreaExpansion}{dt}_{MainStem} \times TN \tag{15}$$

where $\frac{dLeafAreaExpansion}{dt}_{MainStem}$ is the potential leaf area expansion of the main stem and *TN* is the number of tillers. The number of leaves is controlled by the thermal time accumulation and leaf appearance interval or phyllochron (*PHINT*, °C-day). The first leaves of a single plant expand initially at a lower rate due to a low *LAI* and consequently are smaller:

$$\frac{dLeafAreaExpansion}{dt}_{MainStem} = \frac{dLeafAreaExpansion}{dt}_{ActualLeaf} \times \frac{DD}{PHINT} \tag{16}$$

$$\frac{dLeafAreaExpansion}{dt}_{ActualLeaf} = \frac{dLeafAreaExpansion}{dt}_{PreviousLeaf} \times (1 + \Delta LeafAreaExpansion) \tag{17}$$

where *DD* are the accumulated degree-days (°C-day) and $\Delta LeafAreaExpansion$ is the increase of the potential leaf area of the new growing leaf with respect to the previous one (fraction). Actual daily leaf area growth is limited daily by the $\frac{dAgB}{dt}$ times a partitioning coefficient that depends on the development stage of the crop. The model assumes that each tiller can only support four green leaves. $\frac{dLeafAreaLoss}{dt}$ begins in the oldest leaf when the fourth leaf has been developed.

In CropSyst, the actual green area index as a function of time (GAI_t, m^2 m^{-2}) is computed from the actual leaf biomass production ($\frac{dLeaves}{dt}$, kg m^{-2} d^{-1}), the standing leaf biomass ($Leaves_t$, kg m^{-2}) and a partitioning coefficient of the biomass produced to leaves and stem (*LeafStemPart*, m^2 kg^{-1}):

$$\frac{dGAI}{dt} = \frac{\frac{dLeaves}{dt} \times SLA}{(LeafStemPart \times Leaves_t + 1)^2} \tag{18}$$

WOFOST computes *LAI* growth in two stages: (i) an earlier sink limited exponential growth dependent on the daily effective temperature (T_e) and a temperature dependent relative growth rate ($\frac{dLAI}{dt}_{growth,\max}$, (°C-day^{-1})), and (ii) a source limited linear growth that starts once $\frac{dLAI}{dt}_{growth,\max}$ is reached:

$$\begin{cases} (i)\ \dfrac{dLAI}{dt} = LAI_t \times \dfrac{dLAI}{dt}_{growth,\max} \times T_e \\ (ii)\ \dfrac{dLAI}{dt} = \dfrac{dLeaves_t}{dt} \times SLA \end{cases} \tag{19}$$

Canopy senescence can occur due to water stress ($\frac{dLeaves}{dt}_{WS}$), but also when *LAI* gets close to the maximum *LAI* $\frac{dLeaves}{dt}_{HL}$:

$$\begin{cases} \dfrac{dLeaves}{dt}_{WS} = Leaves_t \times \left(1 - \dfrac{T_a}{T_p}\right) \times \dfrac{dLeaves}{dt}_{senH_2O,\max} \\ \dfrac{dLeaves}{dt}_{HL} = Leaves_t \times \dfrac{dLeaves}{dt}_{senHL,\max} \times \dfrac{LAI_t - LAI_{cr}}{LAI_{cr}} \end{cases} \tag{20}$$

where $\frac{dLeaves}{dt}_{senH_2O,\max}$ (kg kg^{-1} day^{-1}) and $\frac{dLeaves}{dt}_{senHL,\max}$ (day^{-1}) are the maximum relative death rate of leaves due to water stress $\left(1 - \frac{T_a}{T_p}\right)$ and due to high *LAI*. The last one is assumed to be 0.03 day^{-1}. LAI_t and LAI_{cr} are the actual and the critical *LAI* (m^2 m^{-2}). LAI_{cr} is the *LAI* required to intercept 95% of the incoming radiation and depends on the light extinction coefficient.

2.1.3. Biomass partitioning and yield formation

In CERES-Wheat, AgB and yield are sink and source limited. Sinks for vegetative biomass and yield are leaves and stems expansion and the number of grains, respectively. Biomass production is the source to fill those sinks and it is mainly driven by intercepted PAR. In WOFOST, the initial leaf area growth is sink-limited. Next to this phase, assimilates are distributed to different organs according to partitioning fractions that change with development stages following a source-limited approach. In Aquacrop and CropSyst, yield simulation depends on total AgB at physiological maturity and a harvest index. The unstressed harvest index is modified according to the water stress with a different intensity depending on the development stage at which the stress occurs.

2.1.4. Soil modules

Different models use alternative methods to calculate the water balance in the soil. They differ in using a descriptive (cascade) or process based (Richards-Darcy) approach, the complexity level with which the soil profile can be described, the soil hydraulic functions and the potential evapotranspiration equations used, and the computation of infiltration, soil evaporation, runoff, drainage and capillary rise. Soil modules are often flexible as they offer alternative approaches according to the user's choice. Table 2 summarizes the equations used in the models and the characteristics of the soil modules as selected for this work. Most important equations defining the different approaches used in each of the studied models are described below.

2.1.4.1. Potential evapotranspiration. Reference evapotranspiration (ET_o) is calculated in the tested models from a variation of Penman's equation (Penman, 1948), with the exception of Aquacrop, where it is provided as input data. CERES-Wheat and CropSyst offer two options (i) FAO56/Penman–Monteith (Allen et al., 1998) and (ii) Priestley–Taylor (Priestley and Taylor, 1972). The first option was selected in both models. WOFOST calculates ET_o based on Penman's equation modified by Frère and Popov (1979) and Penman (1956).

In low-humidity or more arid areas where the aerodynamic term of the Penman equation becomes more important than the energy term, ET_p is underestimated by Penman equation. In FAO56 method (as used in CERES-Wheat and CropSyst) this is corrected based on Doorenbos and Pruitt (1977). However, in WOFOST, this correction is included through the crop coefficient *CFET* ($mm\,mm^{-1}$).

2.1.4.2. Infiltration, drainage and capillary rise. Soil water models can be categorized according to their complexity of process computations and how the soil profile is subdivided (Ranatunga et al., 2008). Most simple models follow a cascading approach: infiltrating water is immediately transferred from one layer to another from the surface towards the subsoil. Rainfall infiltrates or runs off. Water content in a layer increases up to field capacity (*FC*) and when this level is reached, excess water is transferred to the next soil layer (or runs off) until all infiltrated water in that time step is distributed. Cascade-based models might have a single layer or multiple layers. More complex models are based on Richards-Darcy. The soil profile is divided into elements separated by nodes, at which soil water potential and water content are defined.

In the cascade approach of CERES-Wheat, water exceeding field capacity in a soil layer infiltrates to the subsequent layer. This flow is limited by the soil water conductivity at saturation (K_{sat}, $mm\,day^{-1}$). Water flowing from the deeper layer is drained (Eq. (21)):

$$\frac{\partial \theta_t}{\partial t} = K_{sat} \times (\theta_t - \theta_{FC}) \tag{21}$$

where θ_t and θ_{FC} are the soil moisture content at time t and at field capacity ($cm^3\,cm^{-3}$).

In Aquacrop, drainage is quantified according to Barrios-Gonzales (1999), using an empirical drainage characteristic (τ) related to the saturated hydraulic conductivity (K_{sat}). Despite τ given in time units (day^{-1}, as it deduced from Eq. (22)), it characterizes the fraction of drainable water ($cm^3\,cm^{-3}$) lost from a fully saturated soil after one day of free drainage.

$$\frac{\partial \theta_i}{\partial t} = \tau \times \left(\theta_{SAT} - \theta_{FC}\right) \times \left[\left(\frac{e^{\theta_i - \theta_{FC}} - 1}{e^{SAT - \theta_{FC}} - 1}\right)\right] \qquad \tau = 0.0866 \times {K_{sat}}^{0.35} \le 1 \tag{22}$$

where θ_i and θ_{SAT} are the soil moisture content at a specific layer *i* and at saturation ($cm^3\,cm^{-3}$).

In the finite difference approach used in CropSyst, since water flow is based on differences in soil water potential, both downward and upward flow are instantaneously computed. The soil profile is divided into elements separated by nodes, at which soil water potential, water content, and root fractions are defined. This approach solves simultaneously for water transport in the soil and crop water uptake. Water content (θ, $cm^3\,cm^{-3}$) and the hydraulic conductivity are related to soil water potential at each node and the physical properties of the surrounding elements. The rate of change in volumetric water content $\left(\frac{\partial \theta}{\partial t}\text{, in } cm^3\,cm^{-3}\,day^{-1}\right)$, of a soil, both in time and space, is computed with the second order partial differential that is solved for each soil node by Richards' equation (Eq. (23)):

$$\frac{\partial \theta}{\partial t} = \frac{\partial}{\partial z}\left[K(\theta) \times \left(\frac{\partial \varphi}{\partial z} + 1\right)\right] \tag{23}$$

where t is the time (days), z is the soil layer depth (m), $K(\theta)$ is the hydraulic conductivity ($cm\,day^{-1}$) as a function of soil water content and φ is the pressure head (m).

In WOFOST, soil is defined as one homogenous layer that increases at the same rate as rooting depth. Infiltrating water is automatically and homogenously distributed in the whole soil profile, as in a cascade (Eq. (1)).

2.1.4.3. Soil evaporation. In Aquacrop, CERES-Wheat and CropSyst, actual soil evaporation (E_a) is simulated based on a two stages. The first stage is the so-called energy limited stage where E_a is limited by the energy available at the soil surface and continues until a certain soil moisture content (U_{limit}) in the surface layer is reached (Ritchie, 1972). This threshold U_{limit} is determined in Aquacrop by the soil hydraulic characteristics and the depth of the surface layer (Philip, 1957) and can be modified by the user; in CERES-Wheat, U_{limit} is user specified and in CropSyst, U_{limit} is the permanent wilting point (θ_{PWP}) in the first soil layer (Table 2). In the second stage, each model computes E_a on different basis. In Aquacrop, E_a is computed in the second stage based on the relative water content of the upper layer (K_r) (Eqs. (24) and (25))

$$E_a = K_r \times (1 - CC^*) \times K_{ex} \times ET_o \tag{24}$$

$$0 \le K_r = \frac{e^{f_x \times W_{rel}} - 1}{e^{f_x} - 1} \le 1 \tag{25}$$

where K_{ex} is the maximum soil evaporation coefficient (–). In CERES-Wheat, E_a is proportional to the time from where stage 2 started (Eq. (26)).

$$E_a = E_{soil} \times t^{-0.5} \tag{26}$$

where E_{soil} is the potential soil evaporation (mm) (see Table 2 for equation). Lastly, in CropSyst, E_a in stage 2 is computed as in Eq. (27):

$$E_a = E_p \times \frac{\theta_i - \theta_{air\,dry}}{\theta_{FC} - \theta_{air\,dry}} \tag{27}$$

where θ_{airdry} is the soil moisture content is air dry ($cm^3\,cm^{-3}$).

In WOFOST, E_a depends on water surface storage and the infiltration rate and the soil cover (LAI and extinction coefficient) (Eqs. (28)–(31)).

$$E_{p,bare} = ET_o \times e^{-k_{gb} \times LAI} \tag{28}$$

$$\begin{cases} E_a = E_{w,\max} & \text{if } SS_t \ge 1\,\text{cm} \\ E_a = E_{s,\max} & \text{if } SS_t < 1\,\text{cm and } \frac{\partial \theta_i}{\partial t} \ge 1\,\text{cm day}^{-1} \\ E_a = E_{s,\max} \times \left(\sqrt{D_{str}} - \sqrt{D_{str} - 1}\right) & \text{if } \frac{\partial \theta_i}{\partial t} < 1\,\text{cm day}^{-1} \end{cases} \tag{29}$$

$$E_{w,\max} = EO_w \times e^{-k_{gb} \times LAI} \tag{30}$$

$$E_{s,\max} = EO_s \times e^{-k_{gb} \times LAI} \tag{31}$$

where $E_{p,bare}$, EO_w and EO_s are the potential evaporation rate from a bare soil, from a shaded water surface and from a shaded soil surface ($mm\,day^{-1}$), k_{gb} is the extinction coefficient for global radiation (–), $E_{w,max}$ and $E_{s,max}$ are the maximum evaporation rate from a shaded

water surface and from a shaded soil, SS_t is the surface water storage at time t (mm) and D_{slr} are the days since last rain.

2.1.4.4. Runoff. In Aquacrop, CERES-Wheat, and CropSyst, runoff is calculated after a rainfall or irrigation event based on the USDA–SCS curve number approach (USDA, 2004):

$$RO = \begin{cases} 0, & P \le 0.2 \times S \\ \dfrac{(P - I_a)^2}{P - I_a + S}, & P > 0.2 \times S \end{cases} \quad (32)$$

$$S = \frac{1000}{CN} - 10 \quad (33)$$

where RO is the runoff (mm day^{-1}), P is rainfall, I_a is water infiltrated or intercepted by the crop previous to runoff, S is the potential maximum soil moisture retention after runoff begins (mm day^{-1}) and CN is the empirical curve number value (mm^{-1}).

In WOFOST, runoff is based on the maximum surface storage (SS_{max}) of the soil. SS_{max} is user specified (Goudriaan, 1977).

2.1.4.5. Tillage. Tillage is solely explicitly included in CERES-Wheat and CropSyst. Tillage is simulated in CERES-Wheat by adjusting the percentage of surface residues incorporated into the soil, the percentage of soil surface disturbed, the efficiency in soil mixing and the percentage of reduction in the hard pan (White et al., 2009). All these variables compute changes in the bulk density, in the ease of roots to penetrate each of the soil layers or in K_{sat}. CropSyst simulates tillage effects through parameters such as the fraction of soil covered by residues, the fraction of fast cycling, slow cycling and lignified biomass and other parameters related to soil decomposition timing (Sommer et al., 2007). Tillage effects are simulated by changes in runoff, erosion, soil evaporation and the amount of water infiltrating into the soil.

2.1.5. Computation of water stress impact on biomass production

Besides the limitation to biomass growth determined by the potential transpiration of the crop, defined using the WUE coefficient as in the case of CropSyst and Aquacrop, biomass and yields are also reduced when they grow under water deficient conditions. This situation occurs when actual transpiration is lower than the atmospheric demand of water or potential transpiration due to low, easily available soil moisture. Actual transpiration is deemed to be equivalent to water uptake. Crop water uptake is driven by the differences in water potential in the soil and the roots. Aquacrop, CERES-Wheat and WOFOST simplify the process of computing water uptake directly from the easily available water (above the permanent wilting point). CropSyst calculates water potential in the soil based on Campbell (1985). The effect of this water stress is translated into a reduction of biomass growth and yields in each of the studied models following different approaches. Water stress also affects other crop processes such as canopy expansion and partitioning of assimilated carbon. The effects of water stress effects are computed in each of the models as follows.

In Aquacrop, soil water stress is translated into biomass production which affects the expansion of the canopy cover ($K_{s,exp}$), induces both stomata closure ($K_{s,sto}$) and an early canopy senescence ($K_{s,sen}$) and reduces pollination ($K_{s,pol}$) (Raes et al., 2012).

Daily water-limited aboveground biomass production $\left(\frac{dAgB}{dt}_{adj}\right)$ is affected by stomata closure ($K_{s,sto}$) reducing actual transpiration (Eq. (34)):

$$\frac{dAgB}{dt}_{adj} = WP \times \left(\frac{Ta}{ET_o}\right) \times K_{s,sto} \quad (34)$$

Water-limited canopy growth rate and canopy senescence (CGC_{adj} and CDC_{adj}) are affected by $K_{s,exp}$ and $K_{s,sen}$, respectively (Eqs. (35) and (36)).

$$CGC_{adj} = CGC \times K_{s,\exp} \quad (35)$$

$$CDC_{adj} = \left(1 - K_{s,sen}{}^{8}\right) \times CDC \quad (36)$$

Harvest index is affected by $K_{s,pol}$ for water deficit occurring during flowering (Eq. (37)), and by $K_{s,sto}$ when occurring after flowering (Eq. (38)).

$$HI_{adj} = HI_0 \times K_{s,pol} \quad (37)$$

$$HI_{adj} = HI_0 \times \sqrt[10]{K_{s,sto}} \times \left(1 - \frac{1 - K_{s,sto}}{b}\right) \quad (38)$$

where b is a crop parameter that has a lower value if the impact of water deficit on HI is stronger.

The effect of water stress computed in the model is based on soil water content:

$$K_{s,x} = 1 - \frac{e^{S_{rel} \times f_{shape}} - 1}{e^{f_{shape}} - 1} \quad \text{for } K_{s,\exp},\ K_{s,sto} \text{ and } K_{s,sen} \quad (39)$$

$$Ks = 1 - S_{rel} \quad \text{for } K_{s,pol} \quad (40)$$

$$S_{rel} = \frac{\theta_i - \theta_{lower}}{\theta_{upper} - \theta_{lower}} \quad \text{for } \theta_{lower} \le \theta_i \le \theta_{upper} \quad (41)$$

$$\theta_{lower} = \theta_{FC} - (1 - p_{lower}) \times \theta_{WP} \quad (42)$$

$$\theta_{upper} = \theta_{FC} - (1 - p_{upper}) \times \theta_{WP} \quad (43)$$

where S_{rel} is the relative stress level, f_{shape} is a factor determining the convexity of the relation between water stress and available soil moisture; p_{upper} is the fraction of total available water, between wilting point (θ_{WP}, cm^3 cm^{-3}) and field capacity (θ_{FC}, cm^3 cm^{-3}), when water stress starts to affect plant growth and p_{lower} when water stress is at full strength. θ_{lower} equals θ_{WP} for $K_{s,sto}$ and $K_{s,sen}$ When there is no water stress, K_s is set at 1. Otherwise, K_s falls below 1 thus affecting crop transpiration, canopy growth or senescence rate and harvest index.

Water deficit in CERES-Wheat affects the rate of biomass production and canopy senescence (Ritchie, 1998). When potential water uptake decreases to a value lower than the potential transpiration rate, transpiration is reduced by a partial closure of the stomata and the potential biomass production is reduced by the same proportion as the actual to potential transpiration (*SWDF1*) (Eq. (45)). Leaf expansion, branching and tillering are physiological processes especially sensitive to the decrease in turgor pressure due to water deficit, even before stomata closure begins (*SWDF2*). In this sub-routine, turgor pressure is not directly calculated, but it is assumed that the effect of reduced turgor pressure on leaf expansion, branching and tillering begins when the root uptake (T_a) is lower than 1.5 times the potential transpiration (T_p) (Eq. (46)). In CERES-Wheat biomass formation is sink limited, this has a double effect on final yields. Root water absorption is calculated based on the law of the minimum, where the flow rate from soil to roots is dominated by either soil resistance, root resistance or the atmospheric demand of water.

$$U_{CERES,i} = \min\left(q, \frac{2.67 \times 10^{-3} \times e^{62 \times (\theta_t - \theta_{LL})}}{6.68 - \ln(RD_i)}\right) \quad (44)$$

$$SWDF1 = \frac{T_a}{T_p} \quad (45)$$

$$SWDF2 = \frac{T_a}{1.5 \times T_p} \quad (46)$$

where $U_{CERES,i}$ is the daily root water absorption from soil layer i (cm^3 cm^{-1} root day^{-1}), θ_t and θ_{LL} are the soil moisture contents

Table 3
Soil texture and hydraulic characteristics for soil defined with a heterogenous (per horizon) and a homogenous profile (as for WOFOST model).

Texture definition	Horizons	Depth (cm)	Texture (%)			Moisture content (cm cm^{-3}) at pF		Bulk density (g cm^{-3})
			Sand	Silt	Clay	(−1500 kPa)	(−33 kPa)	
Per horizon	**Ap 1**	0–3	21.3	57.6	21.1	0.080	0.240	1.46
	Ap 2	3–25	21.3	57.6	21.1	0.080	0.240	1.46
	Bwy1	25–84	13.8	60.6	25.6	0.100	0.230	1.45
	Bwy2	84–90	9.5	63.3	27.2	0.110	0.270	1.42
Homogenous	–	0–90	16.2	57.9	24.1	0.095	0.235	–

at time t and the lower limit (cm^3 cm^{-3}), and RD_i is the root length density in soil layer i (cm cm^{-3} soil). Root water absorption is restricted to a maximum value (q) of 0.03 cm^3 cm^{-1} root day^{-1}, and if the total water uptake in the soil is higher than the atmospheric demand of water, q is restricted in every soil layer to equal the root water uptake to potential evapotranspiration. Water deficit during the vegetative growth of the crop promotes a shift in partitioning towards roots. This compensates water shortage with a more exhaustive exploration of the soil.

In CropSyst, biomass production rate is reduced in the same proportion as the ratio of actual to potential transpiration. Potential transpiration is calculated as a fraction of the atmospheric demand of water (ET_p) that depends on canopy cover or green area index:

$$T_p = ET_p \times e^{-k \times GAI} \tag{47}$$

where k is a canopy extinction coefficient for solar radiation and GAI is the green area index. Actual transpiration is equated to water uptake assuming no water storage in the plant. It is calculated as described in Stöckle and Jara (1998):

$$U_{CropSyst,i} = K_t \times \frac{C_{ri}}{1.5} \times (\varphi_{si} - \varphi_l) \tag{48}$$

$$C_{ri} = f_1 \times f_{CC} \times C_T \tag{49}$$

$$C_T = \frac{1.5 \times WU_{\max}}{\varphi_{FC} - \varphi_{sto} \times K_t} \tag{50}$$

where $U_{CropSyst,i}$ is the water uptake for soil layer i (kg m^{-2} day^{-1}), K_t is the unit conversion constant (seconds in a day), Cri is the root conductance for the layer i (kg s m^{-4}), φ_l and φ_{si} are the soil layer and canopy average leaf water potential (J kg^{-1} equivalent to m^2 s^{-2}), f1 is the fraction of total root length in layer i (cm cm^{-1}), f_{cc} is the fraction of soil covered by the green canopy (m^2 m^{-2}), WU_{max} is the maximum water uptake (mm day^{-1}); and φ_{FC} and φ_{sto} are the soil water potential at field capacity and the leaf water potential at the onset of stomata closure, respectively. Therefore, the larger the difference between water potential in the soil layer and the plant, the larger the water uptake. The total water uptake is the sum of the U_i from each layer. Water stress also affects crop development and the duration of the green area index in CropSyst. It accelerates the accumulation of degree-days under water stress conditions, as it is assumed that water deficit decreases crop transpiration. A decrease in crop transpiration results in an increase of the temperature inside the canopy resulting in an increase in the effect of the daily accumulation of degree-days.

In WOFOST, water stress reduces gross carbohydrates assimilation (kg CH_2O ha^{-1} day^{-1}) in the same proportion as actual to potential transpiration. Actual transpiration depends on water uptake. Water uptake by the roots is computed taking into account that the resistance to moisture transport increases when soil moisture potential is high (close to wilting point) and decreases when low (close to or at field capacity). In the latter situation, a reduction of transpiration (R_{ws}) is assumed due to water stress. In WOFOST, this reduction in transpiration is calculated as:

$$R_{ws} = \frac{\theta_t - \theta_{WP}}{\theta_{WS} - \theta_{WP}} \quad \text{for } \theta_{WP} \le \theta_t \le \theta_{WS} \tag{51}$$

where θ_t and θ_{WS} are the soil moisture content at time t and a critical soil moisture (cm^3 cm^{-3}), respectively. The last parameter is difficult to measure in trials, and in the model it is calculated as:

$$\theta_{WS} = (1 - p) \times \left(\theta_{FC} - \theta_{WP}\right) + \theta_{WP} \tag{52}$$

where p is the soil water depletion factor (cm^3 cm^{-3}) (similar to easily available water concept in literature) that is a function of potential evapotranspiration rate for a closed canopy and a crop group number (*DEPNR*). This crop group number is a biological factor that determines the relationship between p and potential evapotranspiration (T_p). A high p-factor would (in the limit, maximum 1) give that $\theta_{WS} = \theta_{WP}$, while a low factor would give $\theta_{WS} = \theta_{FC}$. Assuming a homogenous soil with θ_{WP} at 0.095 cm^3 cm^{-3} and θ_{FC} at 0.235 cm^3 cm^{-3} (Table 3) and 6 mm of daily potential transpiration (T_p), the θ_{WS} for each group number can be calculated. Then, a drought sensitive crop belonging to *DEPNR* 1 (e.g. leaf vegetables), p equals 0.23 and θ_{WS}, 0.203; a crop with a medium drought sensitivity belongs to *DEPNR* 3 (e.g. potatoes), p equals 0.40 and θ_{WS}, 0.179; and a drought resistant crop belonging to *DEPNR* 5 (e.g. olive), p equals 0.60 and θ_{WS}, 0.151.

Another parameter indirectly controls the effect of water impact, previously described as crop coefficient (*CFET*). *CFET* (mm mm^{-1}) multiplies the Penman evapotranspiration in such a way that values lower that 1 decrease ET_p, increasing the ratio ET_a/ET_p and decreasing the negative impact of water deficit, and it was intended to adapt the reference *ET* from reference grass to tall crops (Supit et al., 1994).

2.2. Experimental site and data

Observed data was obtained from a long term crop rotation experiment located in Agramunt, Lleida (41° 48′ N, 1° 7′ E, 330 m altitude) in the western area of Catalonia, Spain. The rotation included wheat and barley. Data from seasons in which wheat was grown, 2000–01, 2002–03, 2004–05, 2006–07 and 2011–12, was used. The climodiagram in Fig. 1 depicts the most representative weather station; El Canós (41°41′28″ N, 1°12′13″ E, 429 m). Soil was Typic Xerofluvent (Soil Survey Staff, 1994), silty loam, 0.9 m deep (Table 3), with no groundwater impact on the rooting zone. Soil hydraulic characteristics were obtained in the laboratory using the Richards pressure membrane apparatus.

The experiment was set up in 1990 and originally designed to evaluate the agronomic responses of the crops (growth, yield and its components, water productivity and nitrogen use efficiency) to different management systems based on the reduction of tillage (Cantero-Martínez et al., 2007). Tillage treatments consisted of: (i) mouldboard, intensive ploughing to a depth of 0.3 m, (ii) subsoiling to a depth of 0.5 m, (iii) minimum tillage consisted of a shallow ploughing with a cultivator pass to a depth of 0.15 m, and (iv) no tillage.

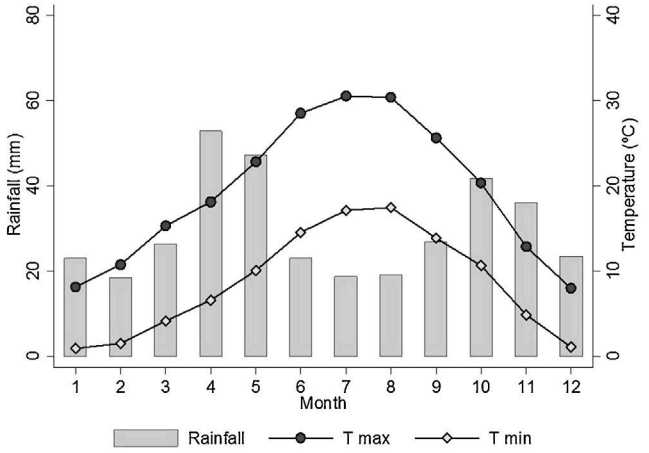

Fig. 1. Climodiagram in El Canós (41°41′28″ N, 1°12′18″ E, 429 masl). Mean monthly data between 2000 and 2013.

Cropping operations, apart from tillage, were similar in all areas. Crops were sown at planting density ranging between 400 and 500 seeds m^2 in 17–19 cm spaced rows. Fertilization was performed according to crop requirements and soil tests. Pig slurry (15–20 m^3 ha^{-1}) was spread before sowing. N mineral fertiliser (50–60 kg N ha^{-1}) was applied on the soil surface before tillering using ammonium nitrate (33.5%). After emergence and before tillering, grass and broadleaf weeds were controlled by herbicide. No treatments were required for pests or diseases.

Only data for no tillage and minimum tillage treatments was selected for this work, as they appeared to be the most effective treatment in increasing yield under the driest conditions in the long term. Moreover, conservation tillage has been widely adopted thus being no tillage and minimum tillage the most representative management. Data on cultivars, sowing, and phenology, yield and aboveground biomass are shown in Table S1.

The experiment was a randomized block design, with 180 m^2 plot size (30 × 6) and treatments were repeated in three blocks. Plant data were collected in each plot at four phenological stages in the first season (2000–01): tillering, jointing, anthesis and physiological maturity; at three phenological stages in the second season (2002–03): jointing, anthesis and physiological maturity; and lastly, at two phenological stages in the remaining seasons (2004–05, 2006–07 and 2011–12): anthesis and physiological maturity. Aboveground biomass was collected by removing all plants from three randomly selected samples of 0.5 m^2 in each plot. Samples were dried to constant weight in a forced-draft oven at 65 °C to obtain dry matter biomass (Cantero-Martínez et al., 2007). Soil water content was measured at two points in each plot and at four depths (0–25, 25–50, 50–75 and 75–90 cm) in the first four seasons and at three depths (0–33, 33–66 and 66–90 cm) in the last season before sowing, at mid-season and after harvest by the gravimetric method (Campbell and Mulla, 1990) by drying to constant weight in a forced-draft oven at 105 °C.

Treatments were repeated in three blocks. Soil water content measured before sowing was different in different blocks (Table S2) and therefore, they were modelled separately to assess the sensitivity of the four models to initial soil water content.

2.3. Models parameterization, calibration and comparison

The parameterization of the models was completed through an iterative process using the observed dates, measured crop growth variables, and default parameters available in the models's crop files. Degree days for different phenological stages were estimated from the base temperature, cutoff temperature and daily mean temperature. Other crop parameters were changed manually around the default parameter values and within a biologically logical range so that simulated yields fitted closer to field observations.

In the first step, parameters related to crop production with neither water or nutrient limitations nor pest and diseases were estimated. As no data to validate the simulated potential yields was available, parameters were selected in such a way that radiation use efficiency and daily potential biomass production were within a physiologically plausible range, and also comparable between models. To compare the models CERES-Wheat, CropSyst and WOFOST in terms of *RUE*, model equations were reproduced in a calculation sheet for a well-established crop during the vegetative growth (no grains yet); 3.5 t ha^{-1} of AgB and a *LAI* of 3.4 were used as inputs. Aquacrop could not be compared in terms of *RUE*, as this model does not base biomass production on radiation but solely on the efficiency of transpired water.

In the second step, parameters for water limited production were calibrated for the trial in season 2000–01 and validated for trials in the remaining seasons. Plots treated with no tillage and with minimum tillage were not differentiated in terms of soil management in the simulation setting as no data on soil changes after tillage was available. Models performance was evaluated using the root mean square error (*RMSE*). This statistic measures the distance between the simulated and the observed values in absolute terms (Eq. (53)). Larger values of *RMSE* indicate decreasing accuracy.

$$RMSE = \sqrt{\frac{\sum_i^n (S_i - O_i)^2}{n}} \tag{53}$$

The impact of water stress on most important crop processes was plotted against soil water availability. The effect on daily aboveground biomass production in each of the models was compared assuming a daily potential evapotranspiration of 6 mm and a daily biomass production of 0.2 t ha^{-1}. The effect on canopy growth and decline rates, and biomass partitioning into grains (harvest index) could only be plotted for Aquacrop; no impact on these two processes is considered in the remaining models.

Weather and soil data was adapted to each of the model formats. Some weather variables coincide (T_{max}, T_{min} and Rainfall) and others are not demanded in all the models (net radiation, wind speed, ET_0 and vapour pressure). Soil moisture content measured at −1500 kPa and at −33 kPa were used in the models as the field capacity and the permanent wilting point. The Penmann–Monteith equation was selected for ET_0 calculation in CERES-Wheat and CropSyst, and the cascade approach for soil water dynamics was selected in CropSyst (no alternatives for Richard-Darcy approach is offered in the remaining models). In CERES-Wheat and CropSyst, soil layers were defined as the horizons shown in Table 3. For potential yield, the simulation option to simulate with no water limitation was used in CERES-Wheat and WOFOST; while an irrigation treatment to keep soil moisture at field capacity was used in Aquacrop and CropSyst.

3. Results and discussion

3.1. Models parameters and approaches

The different approaches used in the models, both in the soil and in the crop modules, make their comparison arduous in terms of soil hydraulic functions and crop parameter values. Models can be compared by (i) isolating computational approaches of a specific crop process; this enables identifying the origin of the different model's performance; or by (ii) comparing outputs, giving an idea on the results that can be expected by the model user. First, model's parameters calibrated for potential production are compared in

Table 4
Crop parameters in Aquacrop, CERES-Wheat, CropSyst and WOFOST crop files.

		Aquacrop	CERES-Wheat	CROPSYST	WOFOST
Biomass production	Extinction coefficient (k, −)	–	0.85	0.6	0.6
	Radiation use efficiency to produce aboveground dry matter (RUE, g MJ^{-1})	–	2.3	2.4	–
	ε, Radiation use efficiency to produce assimilates in a single leaf (kg ha^{-1} h^{-1} J^{-1} m^2 s)	–	–	–	0.45
	Maximum assimilation rate (kg CH_2O ha(leaf)$^{-1}$ h^{-1})	–	–	–	40.00
	Aboveground biomass production per metre of transpired water under given conditions of atmospheric vapour density deficit (K_{BT}) (Pa)	–	–	3.3	–
	Water productivity (WP, g m^{-2})	18	–	–	–
Crop development	LAI_o ($CC_o = 1 - e^{-0.6LAI_o}$)	0.006 (0.4%)	0.4 (21.33%)	0.011 (0.66%)	0.1365 (7.9%)
	LAI_{max} ($CC_{max} = 1 - e^{-0.6LAI_{max}}$)	3.16 (85%)	3.50 (88%)	–	–
	SLA at optimum temperature (m^2 kg^{-1})	–	11.5	22.5	22.5
	GDD[a] end canopy growth (°C-days)	1216	–	1205	–
	GDD[a] begin senescence (°C-days)	1500	–	1500	–
	Days of optimum vernalizing temperature required for vernalization (P1V)	–	60	–	–
	Photoperiod response (% reduction in rate/10 h drop in pp) (P1D)	–	150	–	–
	GDD[a] sowing–emergence (°C-days)	120	–	120	90
	GDD[a] emergence–flowering (°C-days)	1200	–	1200	1200
	GDD[a] anthesis–maturity (°C-days)	460	350	460	490
Yield formation	Kernel number per unit aboveground biomass weight at anthesis (#/g) (G1)	–	19.50	–	–
	Standard kernel weight under optimum conditions (mg) (G2)	–	30.50	–	–
	Standard, non-stressed mature tiller weight (including grain) (g dwt) (G3)	–	2.59	–	–
	DVS1	–	–	–	0.99
	Harvest index	0.45	–	0.5	–

[a] Thermal time is calculated for a base and cutoff temperature of 0 °C and 26 °C, respectively.

terms of radiation use efficiency and water productivity, and discussed. Second, soil water content (cm^3 cm^{-3}) was simulated by each of the four models for a bare soil. As with crop potential production, no data to validate the simulated soil water content with no crop growing on it was available, but it helped in understanding the differences in yield and biomass simulation between models when simulated under water limiting conditions. Soil parameters were the same in each of the models, except for WOFOST, in which *FC* and *PWP* were averaged, as this model assumes a homogenous soil profile (Table 3). Initial soil water conditions were set at the 50% of the plant available water (average between *PWP* and *FC*). Lastly, the relationships defining the impact of water stress on a well-established crop, depending on available soil moisture (cm^3 cm^{-3}) for the four models, are compared. Potential production simulated by the calibrated models, graphs of simulated water-limited versus observed production and soil water contents in time are also presented.

3.1.1. Potential crop biomass production

Crop parameters estimated for potential daily biomass production, canopy development and yield formation in all four studied models are presented in Table 4.

WOFOST is the most detailed model in terms of physiological processes integration as it simulates assimilate production, maintenance requirements of the standing biomass and respiration in the biomass production. All these processes are integrated in CERES-Wheat and CropSyst through a radiation use efficiency parameter.

In WOFOST, the light use efficiency to produce assimilates in a single leaf was set at 0.45 kg CH_2O ha (leaf)$^{-1}$ h^{-1} J^{-1} m^2 s (Table 4). Assimilate production saturates at a maximum rate of assimilates of 40 kg CH_2O ha (leaf)$^{-1}$ h^{-1} (Table 4) (within the range proposed by Boons-Prins et al., 1993) and corresponding to about 59 kg CO_2 ha (leaf)$^{-1}$ h^{-1} (considering a molecular weight of 30 for CH_2O and 44 for CO_2). These values fit closely to the experimentally determined photosynthesis functions shown in Van Keulen and Seligman (1987).

The light extinction coefficient was 0.6 for CropSyst and WOFOST, and differed from the 0.85 set in CERES-Wheat (Table 4). This higher value is due to the fact that leaf area in CERES-Wheat excludes the sheath of the leaves, as authors assume that sheath compared to blade area exposed to light is a constant (Godwin et al., 1989). In CropSyst, the parameter light use efficiency was set at 2.4 g MJ $(PAR)^{-1}$, close to the default value of 2.3 g MJ $(PAR)^{-1}$ set at CERES-Wheat (Table 4). Sinclair and Muchow (1999) reviewed the concept of RUE and calculated it from numerous experiments in the literature for several crops. For wheat, intercepted PAR use efficiency ranged from 1.46 to 2.93 g MJ $(PAR)^{-1}$. The parameter K_{BT} in CropSyst corresponds to the transpiration use efficiency of a crop at a given daily vapour pressure deficit. A large variability for this parameter has been reported in the literature for wheat, ranging from 2.8 to 6.7 Pa (Kemanian et al., 2005). In this work, K_{BT} was set within the reported range, at 3.3 Pa (Table 4).

Potential daily AgB production of a well-established crop against the soil fraction covered by the canopy (Aquacrop) or the photosynthetically active radiation (CERES-Wheat, CropSyst and WOFOST) are contrasted in Fig. 2. Total radiation use efficiency was compared for a well-established crop (3.5 Mg ha^{-1} of AgB, 1.5 Mg ha^{-1} of leaves and 0.4 Mg ha^{-1} of roots, and a LAI of 3.4) in CERES-Wheat, CropSyst and WOFOST in Fig. 2B. RUE was calculated using the linear part of the curve (and in CropSyst when AgB is solely *PAR* limited, Eq. (6)). It resulted in different values for the three models, being higher in CERES-Wheat, followed by CropSyst and lastly

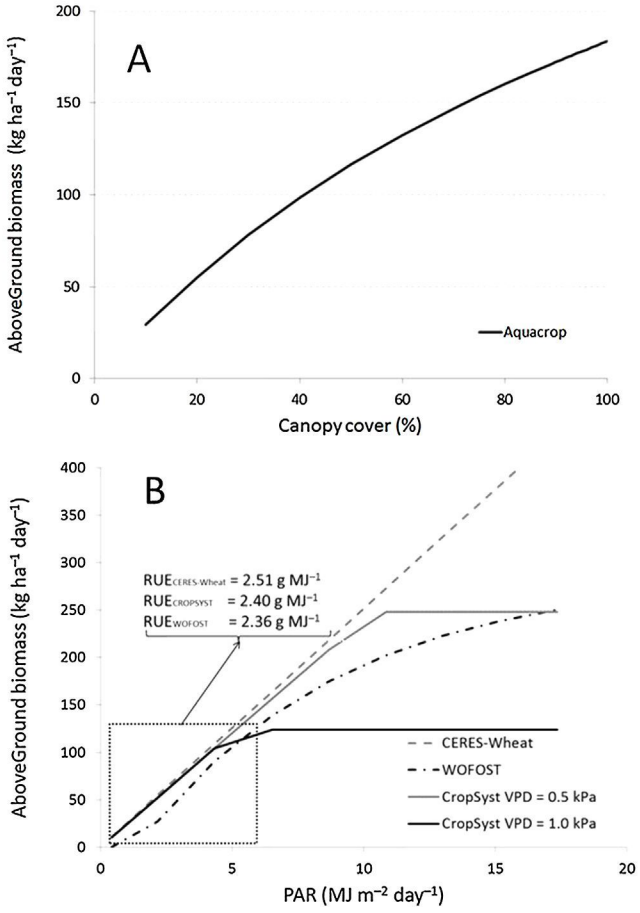

Fig. 2. Aboveground growth rate of biomass (kg ha^{-1} day^{-1}) against (A) soil covered by the canopy (%) and (B) Photosynthetically active radiation (MJ m^{-2} day^{-1}) for a well-established crop (3.5 Mg ha^{-1} of aboveground biomass, 1.5 Mg ha^{-1} of leaves, 0.4 Mg ha^{-1} of roots and a LAI of 3.4) following the approach of the four models under study: (A) in Aquacrop and (B) in CERES-Wheat, WOFOST and CropSyst (for vapour pressure deficit of 0.5 and 1.0 kPa).

WOFOST with 2.51, 2.40 and 2.36 g AgB MJ^{-1} of *PAR*, respectively (Fig. 2B). Taken into account that roots were about 10% of the total biomass, the radiation use efficiency calculated for total biomass results in 2.79, 2.67 and 2.63 g total biomass MJ^{-1} *PAR*. These results are within the range given by Sinclair and Muchow (1999) and described above. In CERES-Wheat, daily biomass production does not saturate at a certain *PAR* (as in CropSyst and WOFOST); biomass growth is sink limited and therefore controlled by a potential daily growth depending on the number of tillers, their developmental stages and the potential tiller weight (parameter G1 in Table 4). The CropSyst equation to compute AgB production from *IPAR* (Eq. (5)) does not saturate at high light levels; nevertheless, the equation that computes AgB production from T_p (Eq. (7)) forces biomass growth to saturate at a maximum rate. This maximum rate fluctuates at each time step as it includes the T_p and *VPD* that vary daily. In Fig. 2B, this variation is shown in the curves for 0.5 and 1.0 kPa of *VPD*. Aquacrop uses a very different approach and therefore it was not possible to compare this model in terms of *RUE*, just the highest rate of daily biomass production in Aquacrop (180 kg dry matter ha^{-1} day^{-1} for a closed canopy) that is lower than the value in WOFOST for high *PAR* (200–250 kg dry matter ha^{-1} day^{-1} for a closed canopy and a *PAR* over 10 MJ m^{-2} day^{-1}) (Fig. 2). The highest rate of daily biomass production in CropSyst is defined by the vapor pressure deficit, for high *PAR*.

In all four models, canopy development has a crucial role in potential biomass production via transpired water in Aquacrop and intercepted radiation in CERES-Wheat, CropSyst and WOFOST (Table 1). Models were quite sensitive to initial conditions and just CC_o in Aquacrop was modified (to 0.4%) (Table 4). LAI_o differed between the remaining models. The lowest value corresponded to CropSyst (0.011), followed by Aquacrop (0.017), WOFOST (0.1367) and lastly by CERES-Wheat (0.4) (Table 4). In CERES-Wheat, canopy growth is sink-limited by the number of tillers and a maximum of four leaves per tiller and a LAI_{max} set internally in the model at 3.5. *SLA* was comparable in CropSyst and WOFOST, 22.5 m^2 kg^{-1}, and it was very low in CERES, 11.5 m^2 kg^{-1}, as it just refers to the blade of the leaves (Table 4). In Aquacrop, *SLA* is not included, but canopy development is driven by thermal time, based on a canopy growth rate and a canopy decline rate in % per °C-day up to CC_{max}, in this case 85% (Table 4).

Thermal time was estimated from phenology data, using sowing, anthesis and physiological maturity dates. In all models, base temperature was 0 °C and cut-off temperature 26 °C. Thermal time between sowing and emergence (120, 120 and 90 °C-days in Aquacrop, CropSyst and WOFOST), between emergence and anthesis (1200 °C-days in Aquacrop, CropSyst and WOFOST) and between anthesis and physiological maturity (460 °C-days) was similar for all four models (Table 4); differences in WOFOST are related to the base temperature to compute thermal time accumulation before emergence. In CERES-Wheat, the time from sowing to anthesis is controlled by the variables *P1V* (vernalization) and *P1D* (photoperiod response). Despite thermal time was similar in all the models, anthesis and physiological maturity are reached in Aquacrop 12 and 11 days before expected (Table 5). A good fit of simulated to observed dates was obtained for 1309 and 477 °C-days from emergence to anthesis and anthesis to maturity, respectively (not shown data). These values are substantially lower to those given by Boons-Prins et al. (1993) for Southern Europe, 1350 and 1000 °C-days; especially the grain filling period.

Yield formation was computed also following alternative approaches. In Aquacrop and CropSyst, yield formation is based on a harvest index that was set to 0.45 and 0.5, respectively (Table 4). In CERES-Wheat, yield formation is sink-limited and determined by the weight of unstressed yield components. Kernel number at anthesis (*G1*) was 19.50 per g of canopy; the standard kernel weight under optimum conditions (*G2*) was 30.50 mg, and the non-stressed mature tiller weight including grain (*G3*), 2.59 g (Table 4). In WOFOST, the parameter *DVS1* refers to the development stage at which assimilates start being accumulated to grain biomass. It was set to 0.99 (Table 4), just before flowering (at *DVS1*) to mimic translocation of assimilates from the vegetative biomass to the grains, a process that was not explicitly included in the model.

Models simulated similar yields under no limiting conditions, to 6 Mg ha^{-1} (Table 5). Results are given as average yields for the calibration and the validation sets, respectively.

3.1.2. Soil water content in bare soil

Soil water content (cm^3 cm^{-3}) was simulated for 1st January to 31st December 2001 with the four models assuming the soil left bare. Average soil water content simulations in the profile and soil water balance are shown in Fig. 3 and Table 6, respectively. Different models show a rather dissimilar performance in terms of the evenness of soil water content changes and of the soil water balance.

Regarding the evenness of the changes in soil water content, WOFOST simulated the sharpest increases and decreases in soil water after rainfall events and in the dry periods, respectively, followed by CERES-Wheat. Aquacrop and Cropsyst simulated more even changes in soil water. This behaviour is the consequence of the number of layers in which the soil is subdivided, a single layer in WOFOST, 5 layers in CERES-Wheat, 12 in Aquacrop and 16 in

Table 5
Model's performance for potential grain yield and aboveground biomass (Mg ha^{-1}) and phenology.

	Plots	N	Observed	Mean				RMSE			
				Aquacrop	CERES	CropSyst	WOFOST	Aquacrop	CERES	CropSyst	WOFOST
Yield (Mg ha^{-1})	Calib set[a]	6	–	6.17	6.48	6.41	6.29	–	–	–	–
	Valid set	24	–	6.45	5.80	5.00	5.83	–	–	–	–
Biomass (Mg ha^{-1})	Calib set	6	–	13.71	17.69	12.81	15.10	–	–	–	–
	Valid set	24	–	14.33	15.86	10.00	13.83	–	–	–	–
Anthesis (average day of the year)	Calib set	6	115.0	104.0	115.0	115.0	115.0	11.0	0.0	0.0	0.0
	Valid set	24	116.5	113.8	121.8	120.8	117.5	12.0	6.8	8.3	9.0
Maturity (average day of the year)	Calib set	6	147.0	140.0	147.0	147.0	147.0	7.0	0.0	0.0	0.0
	Valid set	24	152.0	142.0	150.5	148.8	147.0	11.3	5.0	7.3	8.5

[a] "Calib set": season 2000–2001; "Valid set": remaining seasons.

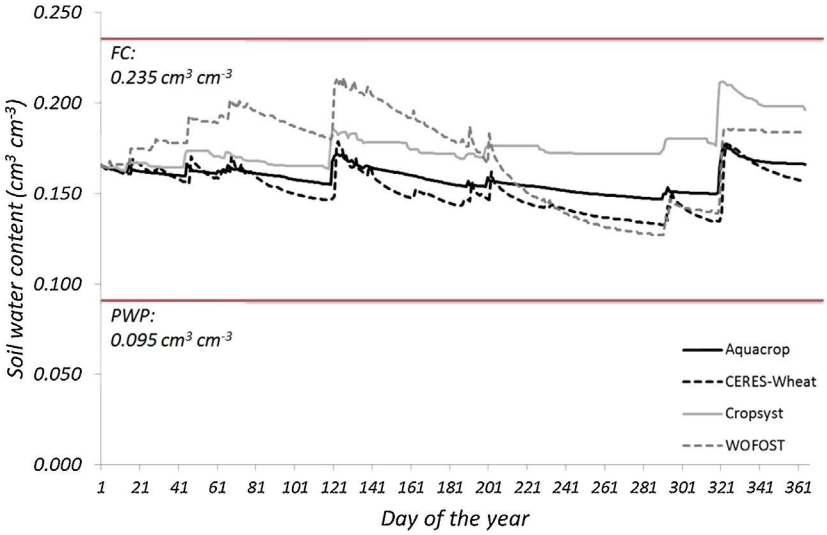

Fig. 3. Soil water content (cm^3 cm^{-3}) for bare soil simulated with Aquacrop, CERES-Wheat, CropSyst and WOFOST between 1st January and 31st December 2001.

CropSyst (Table 2). Therefore, the more layers subdividing the soil profile, the more even the simulated soil water changes.

Rather dissimilar results were found in the soil water balance of different models (Table 6). CERES-Wheat has a negative water balance (−6.16 mm); while it was positive for the remaining models. The lowest increase in soil water was simulated by Aquacrop (+0.45 mm), followed by WOFOST (+17.50 mm) and CropSyst (+27.90 mm). These differences were expected to be due to soil water outputs (soil evaporation, deep drainage and runoff), as all models were supplied with the same weather dataset (rainfall, the sole water input). Soil evaporation was the highest water output in all models. WOFOST simulated the lowest soil evaporation (220.00 mm), followed by CropSyst (224.94 mm), Aquacrop (236.85 mm) and CERES-Wheat (241.72 mm). The comparatively lower soil evaporation in WOFOST than in other models explains why, despite simulating a rather similar increase in total amount of water in the soil as a whole at the moments of a heavy shower (days 121 and 321), in the start of the simulation (up to day 40), with light rainy events, the water content in WOFOST increases more than in the other models. Drainage was nil for all models but for CropSyst, where it was negative (−17.21 mm) despite no water table was considered. This is due to an artefact of the model when using the finite difference approach (as used in this work), the water content of the layer below the defined soil profile is assumed to be equal to the water content of the deepest simulated layer. Then, capillary rise (water upflow) is allowed from the subsoil to satisfy the daily change in soil water when strong gradients develop in the soil profile (Díaz-Ambrona et al., 2005). Finally, runoff was rather low for all models, being nil in WOFOST, 0.20 mm in Aquacrop, 1.87 mm in CropSyst and 1.94 mm in CERES-Wheat.

Hence, the highest change in soil water in CropSyst is explained by the lower soil evaporation and the unexpected water input from the subsoil (negative deep drainage, Table 6). In WOFOST, soil water increase is related to the lower soil evaporation with respect to the remaining models. As no observed data on soil water outputs on the soil left bare was available, it was not possible to determine if actual

Table 6
Soil water balance in Aquacrop, CERES-Wheat, CropSyst and WOFOST from 1st January to 31st December 2001.

	Change	Inputs	Outputs		
	ΔW (mm)	Rainfall (mm)	Soil evaporation (mm)	Drainage (mm)	Runoff (mm)
Aquacrop	+0.45	237.50	236.85	0.00	0.20
CERES-Wheat	−6.16	237.50	241.72	0.00	1.94
CropSyst	+27.90	237.50	224.94	−17.21	1.87
WOFOST	+17.50	237.50	220.00	0.00	0.00

Table 7
Crop parameters related to water deficit as used in CropSyst, WOFOST and Aquacrop.

Parameter	Value
Aquacrop	
Canopy expansion sensitivity	p_{upper}: 0.10; p_{lower}: 0.45; f_{shape}: 5
Stomatal closure sensitivity	p_{upper}: 0.55; f_{shape}: 6
Early canopy senescence sensitivity	p_{upper}: 0.58; f_{shape}: 6
Sensitivity during flowering	p_{upper}: 0.76
Sensitivity after flowering (yield formation) (b)	3
CropSyst	
Leaf water potential at the onset of stomatal closure (J kg^{-1})	−1300
Wilting leaf water potential (J kg^{-1})	−2000
Maximum water uptake (mm day^{-1})	10
Ratio unstressed crop ET/ET$_o$	1 (0.8–1.4)
Leaf area duration sensitivity to water stress	2 (0–3)
Adjustment factor for phenological response to stress	1 (0–1)
WOFOST	
Correction factor transpiration rate	1.1
Crop group number for soil water depletion	3.5

soil evaporation was closer to the simulated one of Aquacrop and CERES-Wheat (about 238 mm) or to the simulated one of WOFOST and CropSyst (about 220 mm); otherwise, soil evaporation could be calibrated by modifying U_{limit} in Aquacrop and CERES-Wheat (as it is user specified), or by modifying the superficial layer depth in CropSyst.

Water input from the subsoil simulated by CropSyst is an important fact to be considered. This "extra" water input can be justified when a wet subsoil below the simulated profile exists and a strong gradient is developed in the rooted soil profile. In these cases, using the finite-difference approach (as in CropSyst in this work), is likely to better simulate actual water dynamics in the soil; however, if no wet subsoil is present, using this approach, an overestimation of soil water content is expected (Díaz-Ambrona et al., 2005).

3.1.3. Sensitivity to soil water deficit

As reviewed by Saseendran et al. (2008), water stress might modify crop development rate, leaf initiation and expansion rate, photosynthesis, carbon allocation and partitioning, and root length and density in soil layers. All four models include the impact of water deficit on crop production but each to a different degree of detail (Table 1).

Parameters related to water stress are shown in Table 7. In Aquacrop, drought resistance is defined for canopy expansion, stomatal closure, flowering and canopy senescence. In CERES-Wheat, parameters related to water deficit effects are based on the ratio potential uptake/potential loss, on soil water content as a fraction of field capacity to permanent wilting point, and the acceleration of leaf area senescence by water shortage. Those parameters are fixed to a species scale and none of them were modified in the calibration. In CropSyst, leaf water potential at the onset of stomatal closure and at wilting point (−1300 and −2000 J kg^{-1}), maximum water uptake (10 mm day^{-1}) and leaf area duration sensitivity to water stress were used to calibrate water limited biomass production (Table 7). In WOFOST, two parameters define the effect of water deficit in water limited biomass production, a correction factor for transpiration rate (*CFET*) and a crop group number for water depletion (*DEPNR*). *CFET* was set at 1.1. *DEPNR* or group number was 3.5; as a moderate drought resistant crop (Table 7).

Fig. 4 shows the curves defining water stress impact on a well-established crop depending on available soil water (cm^3 cm^{-3}) for the four models. Fig. 4A includes the impact of water deficit on

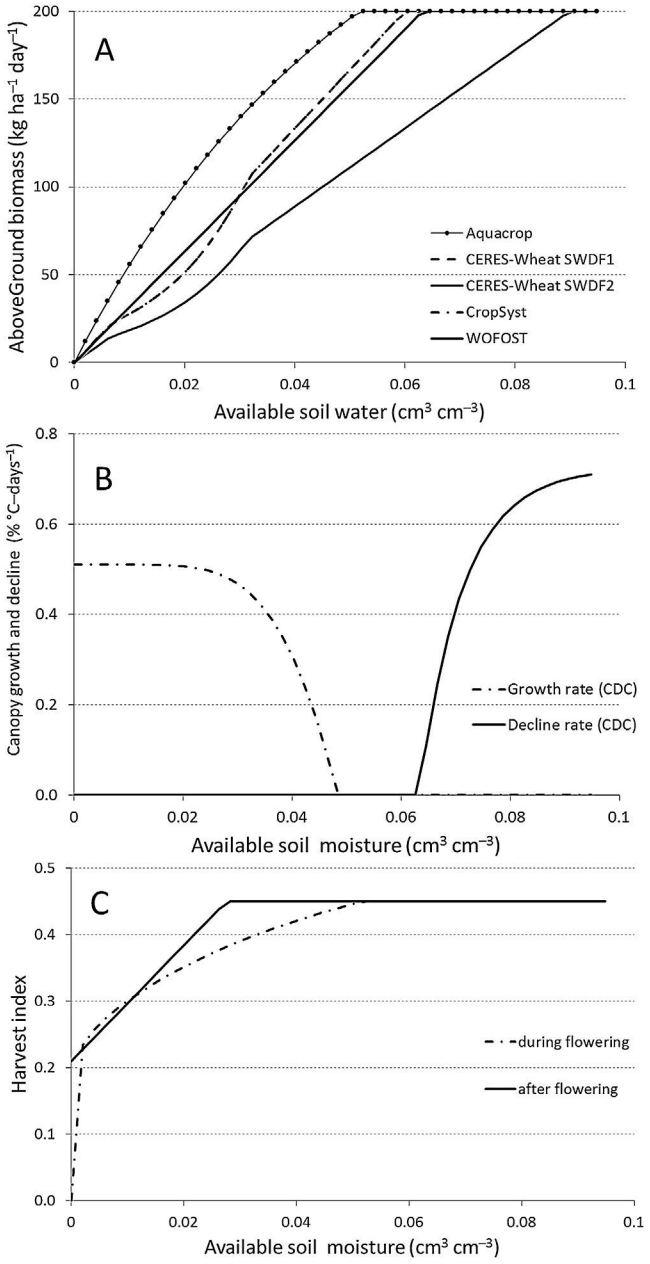

Fig. 4. (A) Aboveground biomass (kg ha^{-1} day^{-1}) in Aquacrop, CERES-Wheat (SWDF1: photosynthesis and transpiration, SWDF2: leaf and stem extension growth and tillering), CropSyst and WOFOST; (B) canopy growth and decline (% °C-day^{-1}) in Aquacrop and (C) harvest index (−) in Aquacrop versus the soil available water ($\theta_t - \theta_{WP}$). At available soil water 0 cm^3 cm^{-3} corresponds to the permanent wilting point at pF = 4.2.

the daily aboveground biomass, assuming a potential production of 200 kg ha^{-1} day^{-1} for CERES-Wheat (*SWDF1* and *SWDF2*), CropSyst and WOFOST. The lowest sensitivity to low soil water availability was found for Aquacrop, followed by CERES-Wheat *SWDF1* and CropSyst and WOFOST. Lastly, CERES-Wheat *SWDF2* (affecting leaf and stem extension growth and tillering, physiological processes especially sensitive to the decrease in turgor) showed a higher sensitivity for the same available water in the soil. As an overall picture, the sensitivity of *SWDF1* and CropSyst are comparable, while the water stress factors affecting different crop processes in Aquacrop, WOFOST and *SWDF2* differ from those and from each other. Fig. 4B shows the canopy growth and decline (% °C-day^{-1}) in Aquacrop. Maximum canopy growth and decline rates were

Table 8
Model's performance for attainable grain yield, mid-season and aboveground biomass (Mg ha^{-1}).

	Plots	*N*	Observed	Mean				RMSE			
				Aquacrop[a]	CERES	CropSyst	WOFOST	Aquacrop	CERES	CropSyst	WOFOST
Yield (Mg ha^{-1})	Calib set[b]	6	2.62	–	1.45	2.62	3.55	–	1.17	0.25	0.93
	Valid set	24	2.55	3.24 (3.00)	2.43	3.08	2.00	1.01	1.13	1.15	1.01
Mid-season AgBBiomass (Mg ha^{-}1)	Calib set	24	3.71	–	3.98	4.66	7.81	–	1.41	1.41	4.10
	Valid set	54	5.81	6.47 (6.94)	5.93	6.33	7.63	2.49	2.99	2.24	2.23
Final AgB Biomass (Mg ha^{-1})	Calib set	6	5.26	–	4.45	5.23	12.36	–	1.15	0.72	7.10
	Valid set	24	6.90	7.20 (8.64)	5.97	6.16	7.30	1.96	1.97	2.02	1.28

[a] Just includes season 2002–03 (all blocks) and season 2011–12 (block 1), as no crop growth was simulated in the remaining cases due to high sensitivity of Aquacrop to low water availability.
[b] "Calib set": season 2000–01; "Valid set": remaining seasons.

obtained by dividing the maximum canopy cover (CC_{max}) by the thermal time for canopy expansion and for canopy decline. Canopy growth is the most sensitive process according to the Aquacrop modelling approach (Fig. 4B). For low water availability, lower than 0.063 cm^3 cm^{-3} (below the permanent wilting point), canopy stops expanding. This high sensitivity to low water availability explains that neither yield nor aboveground biomass was simulated by Aquacrop for most of the seasons (Table 8), those with the lowest initial soil water content before sowing (Table S2).

Fig. 4C shows the negative effect of water deficit on harvest index (no positive effects resulted after calibration). These results suggest that wheat crop is more sensitive to water deficit during flowering and afterwards during the grain filling period.

Observed versus simulated water limited yields, mid-season and at harvest aboveground biomass (Mg ha^{-1}) are presented in Table 8. The limitations of the Aquacrop model to simulate crop growth under the driest conditions prevented the possibility of using the calibration set of observations. The best fit in water limited yields was obtained with CropSyst model (0.26 and 1.25 Mg ha^{-1}, for the calibration and the validation set, respectively), followed by WOFOST (0.95 and 1.44 Mg ha^{-1}) and CERES-Wheat (1.18 and 1.97 Mg ha^{-1}). On the contrary, for aboveground biomass, the best fit was obtained with CERES-Wheat (4.02 and 5.90 Mg ha^{-1}, at mid-season and 5.54 and 5.76 Mg ha^{-1}, at harvest, for the calibration and the validation set, respectively), followed by CropSyst (5.24 and 6.47 Mg ha^{-1}, and 6.19 and 6.27 Mg ha^{-1}) and WOFOST (7.96 and 8.41 Mg ha^{-1}, and 12.89 and 8.65 Mg ha^{-1}). In this last model, aboveground biomass is clearly overestimated, and therefore a low harvest index is calculated.

The effect of water stress on plant development is highly specific to the species and to timing in relation to the growth stages. The inclusion of this effect in a model influences the accuracy in the prediction of the most important phenology dates, and it controls the length of crucial development stages as the grain filling period. WOFOST does not include the effect of water stress on plant development; this might explain the underestimation of the harvest index. Boogaard et al. (2013) found that growth reduction due to drought mainly occurred during the grain filling period in their simulations with WOFOST. On the contrary, the effect of water stress on crop development is directly included in other models. In Aquacrop, water stress lowers the canopy expansion rate (computed separately from biomass growth) and accelerates development (*AQ_CSen*) leading to earlier canopy senescence. In CERES-Wheat, a reduction in biomass production during the vegetative growth of the crop decreases sink strength, and consequently, the relative growth of both vegetative and storage organs are limited. This model also differentiates the strength of water deficit stress depending on the development stage of the crop, being stronger during the exponential growth phase (*SWDF1* and *SWDF2* in Fig. 4A). Crops also respond to water stress with respect to developmental rate (McMaster et al., 2005). In CropSyst, water stress accelerates thermal time accumulation and also modulates leaf area duration promoting earlier canopy senescence.

Plant response to water stress involves physiological changes as stomatal closure that tend to limit water consumption and which result in a reduction of both transpiration and photosynthesis (Farquhar and Sharkey, 1982). Most crop models use a relationship between readily water availability and the ratio of actual to potential transpiration to compute the effect of water deficit on crop growth (Saseendran et al., 2008). This is also the case in the four models studied in this paper. The reduction in the ratio actual to potential transpiration is translated in a lower daily biomass production in Aquacrop, CERES-Wheat and CropSyst and a reduction of daily assimilates production in WOFOST (Table 1).

Changes in the partitioning of carbon allocation and translocation of assimilates to different organs are plant adaptation mechanisms to changes in environmental conditions. Water stress during the vegetative growth of some crops involves a shift in partitioning of assimilates to roots; this helps roots to explore a larger soil volume for water (and nutrients) and increases water uptake to reduce stress (Asseng et al., 1998b). This effect is computed in CERES-Wheat. Flowering is a sensitive stage for many crops (Turner, 2004). Harvest Index (*HI*) is modified in Aquacrop and CropSyst according to water stress. Lastly, water deficits just before reaching maturity might have a positive effect on the *HI* (Geerts and Raes, 2009), this effect is targeted in Aquacrop in an empirical way.

All models implemented the response to water stress in a multiplicative form, based on penalties over the daily assimilates or AgB production, the development rate and the number of flowers pollinated. The difficulty to measure water stress in terms of the effect on individual processes in the crop is the reason for using this empirical approach that cannot be easily justified in terms of biological meaning.

As an overall picture of rainfed crop simulations, rather dissimilar results were output by different models and no good fits were reached in general. *RMSE* in the validation set were higher than 1 Mg ha^{-1} for water limited yields and mostly higher than 2 Mg ha^{-1} for aboveground biomass. This might be explained by the substantial differences in soil water simulations (Tables 9 and 10 and Fig. 5). Soil water in the profile was mostly overestimated in Aquacrop and WOFOST; while this was underestimated in CropSyst. These dissimilarities in soil water simulations are a joint result of the alternative approaches to calculate soil water dynamics used by different models (Table 2) and the differences in crop growth simulations that modifies soil water outputs (mainly through transpiration) affecting soil water content.

The alternative approaches include a different number of layers or sub compartments in the soil for computing the effect of this cascade on the soil water contents and a different detail on soil texture (heterogeneous versus homogenous profile) (Table 2). WOFOST uses a single layer that grows in time with rooting depth

Table 9
Model's performance for soil moisture content ($cm^3\ cm^{-3}$) at two soil depths (0–25 cm and 25–50 cm) and total water available in the rooted soil profile (90 cm) (mm) for Aquacrop, CERES-Wheat and CropSyst.

		Plots	*N*	Observed	Mean			RMSE		
					Aquacrop[a]	CERES	CropSyst	Aquacrop	CERES	CropSyst
Mid-season	$\theta_{0-25\,cm}$ ($cm^3\ cm^{-3}$)	Calib set[b]	6	0.265	–	0.193	0.238	–	0.082	0.027
		Valid set	24	0.211	0.200 (0.255)	0.177	0.207	0.058	0.050	0.033
	$\theta_{25-50\,cm}$ ($cm^3\ cm^{-3}$)	Calib set	6	0.227	–	0.170	0.147	–	0.060	0.073
		Valid set	24	0.179	0.199 (0.219)	0.154	0.149	0.028	0.034	0.035
	Water profile (mm)	Calib set	6	207	–	137	135	–	69	71
		Valid set	24	169	196 (106)	133	143	19	40	27
Harvest	$\theta_{0-25\,cm}$ ($cm^3\ cm^{-3}$)	Calib set	6	0.098	–	0.162	0.187	–	0.073	0.089
		Valid set	24	0.083	0.146 (0.098)	0.125	0.161	0.087	0.077	0.083
	$\theta_{25-50\,cm}$ ($cm^3\ cm^{-3}$)	Calib set	6	0.095	–	0.089	0.099	–	0.012	0.011
		Valid set	24	0.110	0.159 (0.124)	0.123	0.101	0.059	0.037	0.024
	Water profile (mm)	Calib set	6	88	–	95	114	–	25	26
		Valid set	24	94	196 (106)	100	112	103	30	29

[a] Just includes season 2002–03 (all blocks) and season 2011–12 (block 1), as no crop growth was simulated in the remaining cases due to high sensitivity of Aquacrop to low water availability.
[b] "Calib set": season 2000–01; "Valid set": remaining seasons.

Table 10
Model's performance for soil moisture content ($cm^3\ cm^{-3}$) and total water available (mm) in the rooted depth for WOFOST with permanent wilting point (PWP) and field capacity (FC) at 0.095 and 0.235 $cm^3\ cm^{-3}$, respectively. PWP and FC were calculated as the weighted average of the soil water volume at −1500 and −33 kPa, respectively, measured in the laboratory for each soil layer.

		Plots	*N*	Observed	WOFOST	
					Mean	RMSE
Mid-season	$\theta_{profile}$[a] ($cm^3\ cm^{-3}$)	Calib set[b]	6	0.155	0.226	0.082
		Valid set	24	0.184	0.198	0.068
	Water profile (mm)	Calib set	6	207	127	80
		Valid set	24	179	170	12
Harvest	$\theta_{profile}$ ($cm^3\ cm^{-3}$)	Calib set	6	0.066	0.128	0.065
		Valid set	24	0.109	0.137	0.050
	Water profile (mm)	Calib set	6	88	115	27
		Valid set	24	94	123	40

[a] Average soil moisture content in the rooted depth.
[b] "Calib set": season 2000–01; "Valid set": remaining seasons.

and, therefore, it just considers a homogenous textured soil. The other models are more flexible in their structure and allow selecting the number of layers and detail on soil texture. This difference in soil texture leads to different pedotransfer functions.

Transpiration is a key factor driving crop growth. Alternative root distribution modelling approaches (Table 1) leads to differences in simulated crop transpiration and yields in different models. The coincidence of higher soil moisture content with the larger root fraction, leads to a higher water uptake and thus to a higher crop transpiration and biomass production. Moreover, in a layered-soil model there may be higher water content in the top layers, enabling the roots to take up a higher amount of water. This is overlooked by models as WOFOST not simulating root distribution, just rooting depth in one layer assuming water to be homogeneously distributed.

All these interactions seriously hamper a completely separate test, unless data on soil water content on a bare soil is available.

3.2. Critical remarks about the calibration and use of the models

Crop models have a broad field of application in research and engineering. In research, models are used to better understand physiological processes of the crops or interactions between soil, crop and atmosphere. In engineering, crop models are often used to assist policy makers, to foresee the potential impact of changes in management or to quantify resource use requirements and efficiencies.

More careful attention is usually paid to the accuracy of each crop or soil parameter when using crop models within a research perspective, while from an engineering perspective focus is often more output-oriented. Nevertheless, the importance of restricting parameter values to their physiological and/or physical plausible range is evident. Model users solely concerned about model outputs might obtain good fits of model simulations to observed data with a set of parameters with no biological meaning, where an overestimation of some processes compensates the underestimation of others, e.g. too low a LAI might be masked by too high a light extinction coefficient or radiation use efficiency. This would result in the degeneration of the crop model being a very expensive statistical tool.

Despite the existence of both mechanistic and empirical models robust enough to be used for yield prediction and decision support in agriculture, mechanistic models are more adequate to understand the nature of the physiological processes (Yin and Struik, 2010) and to identify crop phenotypes or management strategies to improve yields. In either case, there will always be a certain degree of empiricism due to our limited knowledge of the system, and because the behaviour of the system as a whole (crop–soil–atmosphere) is not always directly explained based on the behaviour of isolated physiological processes (Yin and Struik, 2010). Empirical parameters might also combine in their value some of the errors of other parameters, especially when these are obtained by calibration to best fit model simulations to field observations.

The more a process is modelled with parameters lacking a clear unit, the harder it becomes to determine whether a parameter value is within a justifiable range. Parameters such as SLA or HI have a measurable, physical aspect, which in part depends

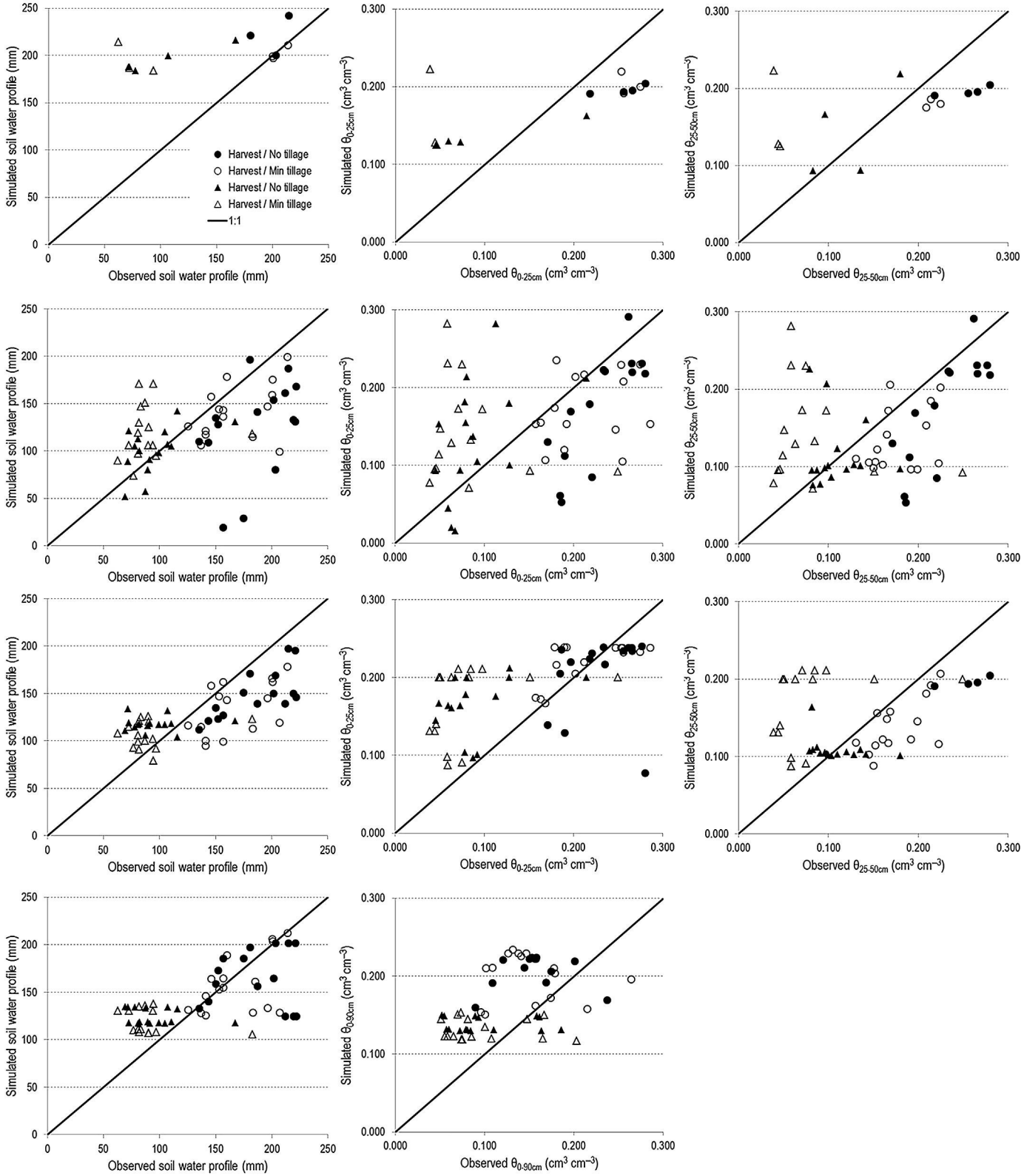

Fig. 5. Observed versus simulated water content in the potential rooting depth (90 cm) (mm), and soil moisture content at two depths (0–25 cm and 25–50 cm), for no tillage (black markers) and minimum tillage (hollow markers), at mid-season (cycles) and at harvest (triangles) for (A) Aquacrop, (B) CERES-Wheat, (C) CropSyst and (D) WOFOST. In WOFOST, the average soil moisture content in the profile was used, as no differentiation in layers is considered in this model.

on sampling expertise; on the contrary, parameters such as the f_{shape} in the curves of sensitivity in Aquacrop are abstract and cannot be measured, but can only be obtained by calibration.

Many uncertainties are also related to soil water simulation. For example, with respect to the assumptions that have to be made on the horizontal heterogeneity of the soils, the effect of tillage, or the criterion used to fix the parameters for permanent wilting

point (*PWP*) and field capacity (*FC*) required in soil modules. Tillage alters soil structure and soil organic matter content (Álvaro-Fuentes et al., 2013; Plaza-Bonilla et al., 2014; White et al., 2009); consequently, it modifies soil water dynamics. Observed data used within this work shows differences in soil water content between the two tillage treatments, being higher in plots with no tillage than in those with minimum tillage, especially in deeper layers ($\theta_{25-50\,cm}$) (Fig. 5). However, model settings for soil management were not differentiated to simulate plots belonging to each of the treatments, as no data on the changes in soil water characteristics were available. The same *FC* and *PWP*, measured at −33 kPa and −1500 kPa using the Richards membranes apparatus, were used. Field capacity is an agronomic concept broadly used by agronomists and soil scientists with still no consensus on its definition. FC refers to the upper limit of the plant available water retained by the soil; it was defined by Veihmeyer and Hendrickson (1931) as the "amount of water remaining in soil after the excess water has drained away and after the rate of downward movement of water has materially decreased", that is one to three days. Nevertheless, this definition is not rigorously defined in physical terms. Numerous operational definitions have been introduced, e.g. based on the matric potential and the drainage rate. Colman (1947) showed that an initially saturated sieved soil after 3 h of internal drainage approaches a matric potential of −33 kPa. It is difficult to define when drainage rate has "materially decreased"; Nachabe (1998) assumed that soil water at *FC* is reached when drainage rate equals 0.05 mm day^{-1}. Anyway, any standardization brings together inaccuracies as it varies with soil texture, soil structure and the organic materials adhered to soil particles; e.g. the pressure values at FC have been reported from −10 to −100 kPa (Cassel and Nielsen, 1986).

It is often the case that no data on a number of variables is available, and the problem of data availability becomes worse as the scale of application is larger; e.g. the increasing heterogeneity of soils in a larger area. In a context with limited observed variables, even when constraining parameter values within their plausible range, model users cannot verify the correctness of the simulation; e.g. in a rainfed cropping system, no data on soil moisture content might lead to compensation of too low a water availability with a higher tolerance of the crop to water deficit and vice versa. This common lack of observed data seriously hampers testing simulation models and thus constitutes an important source of uncertainty. It is then recommended that trials are designed in such a way that most crucial processes in the cropping system are monitored to decrease the probability of incurring these compensating mechanisms. Data used in this work was originally collected to evaluate the effect of alternative tillage systems and therefore variables that would have been of interest regarding the objective of this work lack: e.g., data on plots grown under non-limiting conditions and soil water content dynamics measured on bare soil. Data from plots irrigated according to ET_o would have given a reference of potential yields and AgB (Table 5) and measured (not estimated) values for the parameters shown in Table 4 (such as *RUE*, *WP*, maximum *LAI* or *CC* and phenology under no limiting conditions). Soil water content measured on bare soil would have enabled the separate evaluation of the soil water modules, without the influence of a crop transpiring soil water.

The use of multi-crop model simulations is becoming common in climate change research (e.g. Asseng et al., 2013; Rötter et al., 2011). In this context, these authors propose that simulations of an ensemble of crop models are superior to a single model as errors would tend to cancel each other out. However, according to our experience, the uncertainties associated with a single model are multiplied with a multi-model approach, and averaging multiple model outputs does not contribute to our understanding of the crop–soil–atmosphere system. Data availability to validate model outputs, the degree of model's empiricism, and parameter measurability represent important sources of model uncertainty.

4. Concluding remarks

The different approaches used in the models, both in the soil and in the crop modules, make their comparison arduous in terms of soil hydraulic functions and crop parameter values. For that reason, models were compared by (i) an in-depth analysis of computational approaches of a specific soil and crop process, with the purpose of understanding the reasons of the different model's performance; and by (ii) contrasting model outputs, to orient results towards a more engineering or business use as it gives an idea on what will be expected by the model user. The results suggest that the outputs of the four models for the simulation of winter wheat growth are comparable when water is not limiting, but differences are larger when simulating yields under rainfed conditions. These differences in rainfed yields are mainly related to the dissimilar simulated soil water availability.

This paper answers the questions initially posed.

4.1. Which model(s) is/are preferred from the investigated models?

For the simulation of winter wheat growth at field scale in such semi-arid conditions, CERES-Wheat and CropSyst are preferred. WOFOST is a satisfactory compromise between data availability and complexity when detailed data on soil is limited. Aquacrop integrates physiological processes in some representative parameters, thus diminishing the number of input parameters, what is seen as an advantage when observed data is scarce. However, the high sensitivity of this model to low water availability limits it use in the region considered.

4.2. Is the use of the average of several model's outputs better than the use a single model outputs?

In this paper, models were calibrated in such a way that input parameters (e.g. soil data, thermal time) and variables such as radiation use efficiency and daily potential biomass production were comparable between models. Nevertheless, differences between modelsí outputs are significant when simulating under water-limiting conditions. This suggests that the uncertainties associated with a single model are multiplied with a multi-model approach, and averaging multiple model outputs does not contribute to our understanding of the crop–soil–atmosphere system. Contrary to the use of ensembles of crop models, we endorse that efforts be concentrated on selecting or rebuilding (in case it does not exist) a model that includes approaches that better describe the agronomic conditions of the regions in which they will be applied.

4.3. Given the uncertainties associated to crop model simulations, is it possible to responsibly use crop models in crop insurance analysis and design? If so, what cautions should be taken when using crop model simulations for decision making regarding model(s) calibration and implementation?

The use of such complex methodologies as crop models is associated with numerous sources of uncertainty, although these models are the best tools available to get insight in these complex agronomic systems.

The common lack of observed data seriously hampers testing simulation models and thus constitutes an important source of uncertainty. In order to assess the suitability of crop models for quantifying actual yield variability, a comparison of massive observed actual yields and simulated yields, both on a regional

scale, should be first conducted. Models should preferably be calibrated with data registered in trials specifically designed to obtain parameter values for the selected model.

Acknowledgements

This research was funded by the project MULCLIVAR, from the Spanish Ministerio de Economía y Competitividad (MINECO) CGL2012-38923-C02-02, A. Castañeda-Vera has a PhD grant from UPM. She visited Wageningen University from February to May 2014, where the first discussions on this paper started. We thank Joost Wolf (Wageningen University), Dirk Raes (KU Leuven University) and Tony Hunt (University of Guelph) for the clarifying discussions on WOFOST, Aquacrop and CERES-Wheat models, respectively.

Appendix A. Supplementary data

Supplementary data associated with this article can be found, in the online version, at http://dx.doi.org/10.1016/j.eja.2015.04.008

References

Allen, R.G., Pereira, L.S., Raes, D., Smith, M., 1998. Crop Evapotranspiration: Guidelines for Computing Crop Water Requirements. Rome.

Álvaro-Fuentes, J., Morell, F.J., Madejón, E., Lampurlanés, J., Arrúe, J.L., Cantero-Martínez, C., 2013. Soil biochemical properties in a semiarid Mediterranean agroecosystem as affected by long-term tillage and N fertilization. Soil Tillage Res. 129, 69–74.

Angulo, C., Gaiser, T., Rötter, R.P., Børgesen, C.D., Hlavinka, P., Trnka, M., Ewert, F., 2014. "Fingerprints" of four crop models as affected by soil input data aggregation. Eur. J. Agron. 61, 35–48.

Asseng, S., Anderson, G.C., Dunin, F.X., Fillery, I.R.P., Dolling, P.J., Keating, B.A., 1998a. Use of the APSIM wheat model to predict yield, drainage, and NO_3^- leaching for a deep sand. Aust. J. Agric. Res. 49, 363–378.

Asseng, S., Ewert, F., Rosenzweig, C., Jones, J.W., Hatfield, J.L., Ruane, A.C., Boote, K.J., Thorburn, P.J., Rötter, R.P., Cammarano, D., Brisson, N., Basso, B., Martre, P., Aggarwal, P.K., Angulo, C., Bertuzzi, P., Biernath, C., Challinor, A.J., Doltra, J., Gayler, S., Goldberg, R., Grant, R., Heng, L., Hooker, J., Hunt, L.A., Ingwersen, J., Izaurralde, R.C., Kersebaum, K.C., Müller, C., Naresh Kumar, S., Nendel, C., O'Leary, G., Olesen, J.E., Osborne, T.M., Palosuo, T., Priesack, E., Ripoche, D., Semenov, M.A., Shcherbak, I., Steduto, P., Stöckle, C., Stratonovitch, P., Streck, T., Supit, I., Tao, F., Travasso, M., Waha, K., Wallach, D., White, J.W., Williams, J.R., Wolf, J., 2013. Uncertainty in simulating wheat yields under climate change. Nat. Clim. Change 3, 827–832.

Asseng, S., Ritchie, J.T., Smucker, A.J.M., Robertson, M.J., 1998b. Root Growth and Water Uptake During Water Deficit and Recovering in Wheat., pp. 265–273.

Barrios-Gonzales, J.M., 1999. Comparative Study of Three Approaches in the Computation of Soil Water Balance.

Basso, B., Cammarano, D., Carfagna, E., 2013. Review of crop yield forecasting methods and early warning systems abstract. In: First Meeting of the Scientific Advisory Committee of the Global Strategy to Improve Agricultural and Rural Statistics. FAO Headquarters, Rome, Italy, pp. 1–56.

Boogaard, C.A., Van Diepen, R.P., Rötter, J.M.C.A., Cabrera, H.H., VanLaar, H.L., DeWit, H.L., TeRoller, J.A., 2011. WOFOST Control Centre 1.8 and WOFOST 7.1.3. Wageningen.

Boogaard, H., Wolf, J., Supit, I., Niemeyer, S., van Ittersum, M., 2013. A regional implementation of WOFOST for calculating yield gaps of autumn-sown wheat across the European Union. Field Crop. Res. 143, 130–142.

Boons-Prins, E.R., de Koning, G.H.J., van Diepen, C.A., Penning de Vries, F.W.T., 1993. Crop Specific Simulation Parameters for Yield Forecasting Across the European Community (No. 32), Simulation Reports CABO-TT. Wageningen, The Netherlands.

Campbell, G.S., 1985. Soil Physics with BASIC: Transport Models for Soil–Plant Systems. Elsevier, Amsterdam.

Campbell, G.S., Mulla, D.J., 1990. Measurement of soil water content and potential. Irrig. Agric. Crop., p127–p141.

Cantero-Martínez, C., Angás, P., Lampurlanés, J., 2007. Long-term yield and water use efficiency under various tillage systems in Mediterranean rainfed conditions. Ann. Appl. Biol. 150, 293–305.

Cassel, D.K., Nielsen, D.R., 1986. Field capacity and available water capacity. In: Klute, A. (Ed.), Methods of Soil Analysis. Part 1: Physical and Mineralogical Methods. American Society of Agronomy and Soil Science Society of America, Madison, pp. 901–926.

Colman, E.A., 1947. A laboratory procedure for determining the field capacity of soils. Soil Sci., 277.

Díaz-Ambrona, C.G.H., O'Leary, G.J., Sadras, V.O., O'Connell, M.G., Connor, D.J., 2005. Environmental risk analysis of farming systems in a semi-arid environment: effect of rotations and management practices on deep drainage. Field Crop. Res. 94, 257–271.

Doorenbos, J., Pruitt, W.D., 1977. Guidelines for Predicting Crop Water Requirements (No. 24), Irrigation and Drainage. Rome, Italy.

Farquhar, G.D., Sharkey, T.D., 1982. Stomatal conductance and photosynthesis. Annu. Rev. Plant Physiol. 33, 317–345.

Frère, M., Popov, G.S., 1979. Agrometeorological Crop Monitoring and Forecasting (No. 17), Plant Production and Protection. Rome.

Geerts, S., Raes, D., 2009. Deficit irrigation as an on-farm strategy to maximize crop water productivity in dry areas. Agric. Water Manag. 96, 1275–1284.

Godwin, D., Ritchie, J., Singh, U., Hunt, L., 1989. A User's Guide to CERES Wheat – V2.10. Alabama.

Goudriaan, J., 1986. A simple and fast numerical method for the computation of daily totals of crop photosynthesis. Agric. For. Meteorol. 38, 249–254.

Goudriaan, J., 1977. Crop Micrometeoroogy: A Simulation Study. Centre for Agricultural Publishing and Documentation, Wageningen, the Netherlands.

Hoogenboom, G., Jones, J.W., Wilkens, P.W., Porter, C.H., Boote, K.J., Hunt, L.A., Singh, U., Lizaso, J.L., White, J.W., Uryasev, O., Royce, F.S., Ogoshi, R., Gijsman, A.J., Tsuji, G.Y., Koo, J., 2012. Decision Support System for Agrotechnology Transfer (DSSAT) Version 4.5 [CD-ROM].

Hunt, J., Van Rees, H., Hochman, Z., Carberry, P., Holzworth, D., Dalgliesh, N., Poulton, P., Van Rees, S., Huth, N., Peake, A., 2006. Yield Prophet®: An online crop simulation service. In: Ground Breaking Stuff. Proceedings of the 13th ASA Conference, Perth, Western Australia., pp. 1–5.

Jones, J., Hoogenboom, G., Porter, C., Boote, K., Batchelor, W., Hunt, L., Wilkens, P., Singh, U., Gijsman, A., Ritchie, J., 2003. The DSSAT cropping system model. Eur. J. Agron. 18, 235–265.

Kemanian, A.R., Stöckle, C.O., Huggins, D.R., 2005. Transpiration-use efficiency of barley. Agric. For. Meteorol. 130, 1–11.

Kersebaum, K.C., Hecker, J., Mirschel, W., Wegehenkel, M., 2007. Modelling water and nutrient dynamics in soil–crop systems: a comparison of simulation models applied on common data sets. In: Modelling Water and Nutrient Dynamics in Soil–Crop Systems. Springer, Dordrecht, pp. 1–17.

Martre, P., Wallach, D., Asseng, S., Ewert, F., Jones, J.W., Rötter, R.P., Boote, K.J., Ruane, A.C., Thorburn, P.J., Cammarano, D., Hatfield, J.L., Rosenzweig, C., Aggarwal, P.K., Angulo, C., Basso, B., Bertuzzi, P., Biernath, C., Brisson, N., Challinor, A.J., Doltra, J., Gayler, S., Goldberg, R., Grant, R.F., Heng, L., Hooker, J., Hunt, L.A., Ingwersen, J., Izaurralde, R.C., Kersebaum, K.C., Müller, C., Kumar, S.N., Nendel, C., O'Leary, G., Olesen, J.E., Osborne, T.M., Palosuo, T., Priesack, E., Ripoche, D., Semenov, M.A., Shcherbak, I., Steduto, P., Stöckle, C.O., Stratonovitch, P., Streck, T., Supit, I., Tao, F., Travasso, M., Waha, K., White, J.W., Wolf, J., 2014. Multimodel ensembles of wheat growth: many models are better than one. Glob. Change Biol. 21, 911–925.

McMaster, G.S., Wilhelm, W.W., FranK, A.B., 2005. Developmental sequences for simulating crop phenology for water-limiting conditions. Aust. J. Agric. Res. 56, 1277–1288.

Nachabe, M.H., 1998. Refining the definition of field capacity in the literature. J. Irrig. Drain. Eng., 230–232.

Penman, H.L., 1948. Natural evaporation from open water, bare soil and grass. Proc. R. Soc. Lond. 193, 120–145.

Penman, H.L., 1956. Evaporation: an introductory survey. Netherlands J. Agric. Sci., 9–29.

Philip, J.R., 1957. Evaporation, and moisture and heat fields in the soil. J. Meteorol. 14, 354–366.

Plaza-Bonilla, D., Álvaro-Fuentes, J., Cantero-Martínez, C., 2014. Identifying soil organic carbon fractions sensitive to agricultural management practices. Soil Tillage Res. 139, 19–22.

Priestley, C.H.B., Taylor, R.J., 1972. On the assessment of surface heat flux and evaporation using large-scale parameters. Mon. Weather Rev. 100, 81–92.

Raes, D., Steduto, P., Hsiao, T.C., Fereres, E., 2009. AquaCropThe FAO crop model to simulate yield response to water: II. Main algorithms and software description. Agron. J. 101, 438–447.

Raes, D., Steduto, P., Hsiao, T.C., Fereres, E., 2012. Calculation procedures. In: Aquacrop v4.0 Reference Manual. Rome., pp. 130.

Ranatunga, K., Nation, E., Barratt, D., 2008. Review of soil water models and their applications in Australia. Environ. Model. Softw. 23, 1182–1206.

Rinaldi, M., Ventrella, D., Gagliano, C., 2007. Comparison of nitrogen and irrigation strategies in tomato using CROPGRO model. A case study from Southern Italy. Agric. Water Manag. 87, 91–105.

Ritchie, J.T., 1972. Model for predicting evporation from a row crop with incomplete cover. Water Resour. Res. 8, 1204–1213.

Ritchie, J.T., 1998. Soil water balance and plant water stress. In: Tsuji, G.Y., Hoogenboom, G., Thornton, P.K. (Eds.), Understanding Options for Agricultural Production. Kluwer Academic Publishers and International Consortium for Agricultural Systems Applications, Dordrecht, The Netherlands, pp. 41–54.

Rötter, R.P., Carter, T.R., Olesen, J.E., Porter, J.R., 2011. Crop – climate models need an overhaul. Nat. Clim. Change 1, 175–177.

Saseendran, S.S., Ahuja, L.R., Ma, L., Boote, K.J., Hoogenboom, G., 2008. Current water deficit stress simulations in selected agricultural system models. In: Response of Crops to Limited Water: Understanding and Modeling Water Stress Effects on Plant Growth Processes., pp. 1–38.

Sinclair, T.R., Muchow, R.C., 1999. Radiation use efficiency. Adv. Agron. 65, 215–265.

Soil Survey Staff, 1994. Keys to Soil Taxonomy. Washington, DC, USA.

Sommer, R., Wall, P.C., Govaerts, B., 2007. Model-based assessment of maize cropping under conventional and conservation agriculture in highland Mexico. Soil Tillage Res. 94, 83–100.
Steduto, P., Hsiao, T.C., Fereres, E., Raes, D., 2012. Crop Yield Response to Water (No. 66). FAO Irrigation and Drainage, Rome.
Stöckle, C.O., Jara, J., 1998. Modeling transpiration and soil water content from a corn (*Zea Maize* L.) field: 20 min vs. daytime integration step. Agric. For. Meteorol. 92, 119–130.
Stöckle, C.O., Donatelli, M., Nelson, R., 2003. CropSyst, a cropping systems simulation model. Eur. J. Agron. 18, 289–307.
Supit, I., Hooijer, A.A., van Diepen, C.A., 1994. System description of the WOFOST 6.0 Crop Simulation Model Implemented in CGMS. Volume 1: Theory and Algorithms (No. EUR 15956 EN), An Agricultural Information System for the European Community. Luxemburg.
Turner, N.C., 2004. Agronomic options for improving rainfall-use efficiency of crops in dryland farming systems. J. Exp. Bot. 55, 2413–2425.
USDA, 2004. Estimation of direct runoff from storm rainfall. In: National Engineering Handbook. U.S. Department of Agriculture (USDA), pp. 1–51.
Van Ittersum, M.K., Cassman, K.G., Grassini, P., Wolf, J., Tittonell, P., Hochman, Z., 2013. Yield gap analysis with local to global relevance—a review. Field Crop. Res. 143, 4–17.
Van Keulen, H., Seligman, N.G., 1987. Simulation of Water Use, Nitrogen Nutrition and Growth of a Spring Wheat Crop. Centre for Agricultural Publishing and Documentation, Wageningen, The Netherlands.
Veihmeyer, F.J., Hendrickson, A.H., 1931. The moisture equivalent as a measure of the field capacity of soils. Soil Sci., 181–194.
Ventrella, D., Charfeddine, M., Giglio, L., Castellini, M., 2012. Application of DSSAT models for an agronomic adaptation strategy under climate change in Southern of Italy: optimum sowing and transplanting time for winter durum wheat and tomato. Ital. J. Agron. 7, 109–115.
White, J.W., Jones, J.W., Porter, C., McMaster, G.S., Sommer, R., 2009. Issues of spatial and temporal scale in modeling the effects of field operations on soil properties. Oper. Res. 10, 279–299.
Yin, X., Struik, P.C., 2010. Modelling the crop: from system dynamics to systems biology. J. Exp. Bot. 61, 2171–2183.